MoDOT

PB2000-100890

Research, Development and Technology Division

University of Missouri-Rolla

RDT 99-005
Final Report

Manufacture and Performance Evaluation of FRP Rebar Featuring Ductility and Health Monitoring Capability

RI97-012

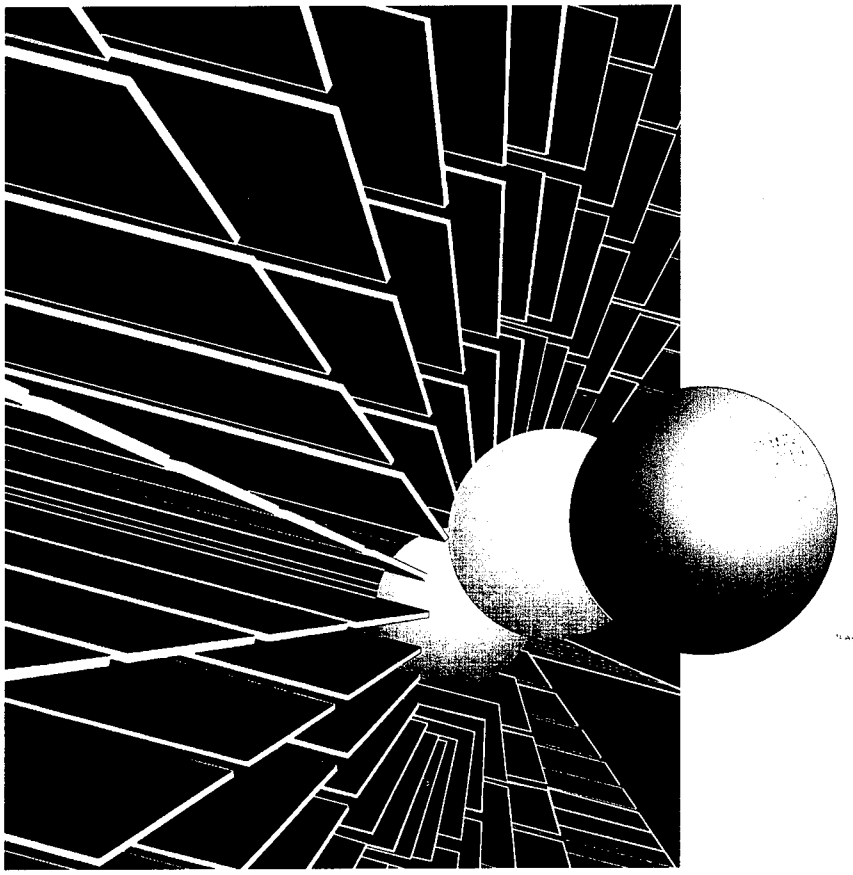

June, 1999

TECHNICAL REPORT DOCUMENTATION PAGE

1. Report No. RDT 99-005	2. Government Accession No.	3. Recipient's Catalog No.
4. Title and Subtitle Manufacture and Performance Evaluation of FRP Rebar Featuring Ductility and Health Monitoring Capability		5. Report Date June 1999 6. Performing Organization Code UMR
7. Author(s) Abdeldjelil Belarbi, K. Chandrashekhara and Steve E. Watkins		8. Performing Organization Report No. RDT 99-005
9. Performing Organization Name and Address University of Missouri-Rolla 1870 Miner Circle Rolla, MO 65409		10. Work Unit No. 11. Contract or Grant No.
12. Sponsoring Agency Name and Address Missouri Department of Transportation Research, Development and Technology Division P. O. Box 270 Jefferson City, MO 65102		13. Type of Report and Period Covered Final Report 14. Sponsoring Agency Code MoDOT

15. Supplementary Notes

The investigation was conducted in cooperation with the U. S. Department of Transportgation, Federal Highway Administration.

16. Abstract

The main objective of this study was to develop a new type of FRP rebar with focus on ductility and health-monitoring issues. One approach to provide ductility was the use of a hybrid FRP reinforcing bar consisting of different types of fibers, which fail at different strains during the load history of the rebar, thereby allowing a gradual failure of the rebar. The Manufacturing of the rebar was achieved by pultrusion and filament winding techniques. These techniques have made it possible to embed fiber optic sensors within the reinforcement, for health monitoring, thus protecting the sensor from the harsh concrete environment. Pseudo-ductile behavior was validated through testing of coupon FRP rebar as well as RC beams. Testing of large-scale beams reinforced with theis hybrid FRP rebar exhibited remarkable ductility behavior with ductility indices close to that of beams reinforced with steel rebar. Furthermore, the strain measured from the embedded fibers optics replicates the measurement of conventional LVDT and was reliable up to failure of the beams.

17. Key Words	18. Distribution Statement
Composite, Ductility, Fiber Reinforced Polymer (FRP), Flexure, Health Monitoring, Reinforced Concrete Beams, Reinforcing Bars (Rebar), Sensors (Strain)	No restrictions. This document is available to the public through National Technical Information Center, Springfield, Virginia 22161

19. Security Classification (of this report)	20. Security Classification (of this page)	21. No. of Pages	22. Price
Unclassified	Unclssified		

Manufacture and Performance Evaluation of FRP Rebar Featuring Ductility and Health Monitoring Capability

FINAL REPORT

RDT 99-005

PREPARED BY

UNIVERSITY OF MISSOURI-ROLLA

By

A. Belarbi
Department of Civil Engineering

K. Chandrashekhara
Mechanical & Aerospace Engineering & Engineering Mechanics

S.E. Watkins
Electrical & Computer Engineering

June 1999

ACKNOWLEDGEMENTS

Funding of this project was shared by Missouri Department of Transportation (MoDOT), Mid-America Transportation Center (MATC) and Manufacturing Research and Training Center (MRTC) at the University of Missouri-Rolla. Their support is gratefully acknowledged.

TABLE OF CONTENTS

ABSTRACT

A suitable replacement for steel reinforcing to be used in reinforced concrete structures is presented. Steel reinforcing corrodes with time, thus reducing the capacity of a reinforced concrete structure. Composite fiber reinforced plastic (FRP) reinforcing has been used in some concrete structures as a replacement for steel; however, this corrosion resistant replacement comes at the cost of ductility to the structure. Current manufacturers fabricate FRP reinforcing which is linear elastic (or brittle) until failure.

One solution to provide ductility is a hybrid FRP reinforcing bars. The proposed hybrid rebar consists of different types of fibers which fail at different strains during the load history of the rebar, thereby allowing a gradual failure of the rebar. In addition to different types of fibers, different manufacturing techniques can be applied to help obtain some additional ductility. Using the pultrusion and filament winding techniques, FRP reinforcing with pseudo-ductility was developed and tested. The application of these two manufacturing techniques has also made it possible to embed fiber optic sensors within the reinforcing, thus protecting the sensor from the harsh concrete environment. Fiber optic sensors provide real time monitoring of the structure for extended periods of time.

Pseudo-ductile behavior was proven through various tensile coupon tests on hybrid FRP rebars; the observed behavior closely matched that of a concrete stiffened steel rebar. Furthermore, the performance of hybrid FRP rebars embedded in concrete beams also indicated pseudo-ductile behavior which was evaluated by experimental moment curvature diagrams as well as load deflection curves. Furthermore, the strain measured from the embedded fibers optics replicates the measurement of conventional LVDT and was reliable up to failure of the beams. Bond tests revealed that sand-coated rebars have adequate bond resistance at the concrete-rebar interface.

LIST OF ILLUSTRATIONS

Figure Page

LIST OF TABLES

I. INTRODUCTION

A. GENERAL

Limited service life and high maintenance costs are associated with corrosion, fatigue, and other degradations in bridge and highway structures. Repair and replacement cost factors have led highway agencies and researchers to investigate new concepts applying advances in materials technology. For many years, reinforced concrete (RC) has been the material of choice for structures due to its ease of design, cost, and availability. However, corrosion of steel embedded in concrete is a major cause of widespread and accelerated deterioration in reinforced concrete structures.

In the late 1970s, the Federal Highway Administration performed extensive testing of various corrosion protection methods with limited success. These methods included using highly impermeable concrete, applying penetrating sealers, using epoxy-coated reinforcement, cathodic protection, and incorporating corrosion inhibitors. Current efforts to improve transportation and civil infrastructures include the use of high-performance composite materials. Composites, consisting of fibers embedded in a matrix, are used extensively in aerospace and automotive industries. Most of the current research using composites for civil applications deals with the rehabilitation and reinforcement of existing concrete structures [1]. Some research has been performed to fabricate whole structural elements such as pipe, poles, and building members from composites, while fiberglass rebars and prestressing tendons have been developed for use in reinforced and prestressed concrete applications. Fiber reinforced plastic (FRP) rebars and tendons are not commonly used in structural design because of insufficient bond

resistance, poor bend-up capabilities, and nonexistent ductility which are fundamental requirements of rebar in RC structural design.

Within the last 25 years, fiber composites have entered the civil engineering community in the form of FRP reinforcing for reinforced or prestressed concrete structures. However, in the last few years civil engineers have begun to fully realize the benefits of FRP reinforcing. Not only is FRP currently used in some new construction, but it can also be applied in retrofitting existing structures to withstand seismic disturbances or to increase capacity [1]. Also, with the advent of smart structural systems, it is possible to successfully embed fiber optic sensors within the FRP to monitor a structural response at any time. Fiber optic sensors provide real time monitoring of the concrete structure for extended periods of time. In the future, embedded sensors will be coupled with active damping systems to reduce vibration and subsequent damage to a structure.

Because of deficiencies in available FRP rebars, current research has been focused on developing a new type of composite rebar for RC use. This composite rebar would be corrosion resistant. In addition, the mechanical properties of composites can be tailored for specific applications. It would meet all the requirements imposed on conventional rebar, such as strength, stiffness, ductility, fatigue, bond, and bent-up capabilities. Furthermore, it will offer "smart" capability in which embedded sensors, e.g., fiber optic sensors, provide health monitoring and micro-damage assessment without destructive evaluation. Composite rebar would be primarily used in structures threatened by corrosion such as highway bridges, bridge decks, marine structures, deep foundations, and other structures in which health monitoring is desirable.

B. FRP REBARS

Fiber reinforced composites consist of fibers embedded in a matrix material. The matrix binds the fibers together, transfers loads to the fibers, and protects the fibers. Most FRP manufacturers produce reinforcing using a glass fiber and resin system. From the cost perspective glass fibers show the most promise, since they are the least expensive and are readily available. However, from the design and serviceability perspective, glass fiber FRP does not have the stiffness or the stress requirements of conventional steel reinforcing. In many cases, glass fiber reinforced concrete under-utilizes both materials involved and thereby adds to the cost of the project. Other manufacturers are beginning to use carbon fibers instead of glass fibers, especially in prestressed applications. While carbon fibers can have a stiffness comparable to that of steel, this stiffness is often achieved at high stress levels which are not applicable to conventional reinforced concrete structures.

1. Ductility Issue in Fiber Reinforced Plastics. One issue FRP manufactures do not address is the requirement of ductility in FRP reinforced structural systems. Current FRP rebars are linear elastic until failure in contrast to steel which has a definite yielding plateau. By definition, ductility is an increase in deformation without an increase in capacity. In traditional reinforced concrete structures, ductility is provided by the yielding of longitudinal steel reinforcement. The yielding of reinforcement is then translated as excessive deformations in the concrete structure. Excessive deformations give warning to the occupants that failure of the structure is near. In fiber composites, there is no definite yield point, since most fibers are linear elastic until failure [2]. As a

result, fiber composites exhibit brittle behavior which, if used in a reinforced concrete system, would give no warning of structural failure.

In terms of current reinforced concrete design codes, linear elastic FRP rebars are unacceptable since no ductility is evident. The design philosophy of current RC code is based entirely on the requirement of yielding in the steel reinforcing. Throughout history, this design philosophy has been economical and reliable. Researchers have realized that an economical and reliable structure can not be designed using FRP and current RC design codes, and thus many different solutions have been proposed. The best solution would be to incorporate ductility within the FRP rebar. This is advantageous because the current reinforced concrete design codes could then be used for either steel or FRP reinforcing. In addition, structural engineers would not be required to learn new design codes for FRP reinforcing.

A second alternative to FRP RC design would be to custom tailor a design philosophy based on the engineering properties of linear elastic FRP reinforcing. In other words, additional safety in a structure could be provided by additional capacity instead of ductility. Many drawbacks are related to this alternative, with the most obvious being the economic issue. Typically, to provide additional capacity in a structure more material is required; this in turn increases the cost of the structure. Furthermore, structural engineers would be required to possess knowledge in the FRP design code as well as traditional RC design code.

2. Health Monitoring in Civil Engineering. Health monitoring, or the ability to measure a structure's response over time can give valuable information about a structure [3]. Many different methods have been used in the past to collect this information: load

cells, strain gages, and linear variable differential transformers (LVDT) are the most common. Load cells can be placed under the supports of a structure to measure the total load, or reaction. Strain gages and LVDT's are used to measure strain and deflection at a specific point. Due to their small gage length, strain gages measure the strain at a localized point on the structure. In contrast, the gage length of a LVDT can be quite large, thus providing an average strain reading for the structure. These methods are effective for short term monitoring or load testing, but a different approach must be used for long term monitoring. Long term monitoring requires instruments that are reliable, cost-effective, and protected from the environment. In addition, the instrumentation must not impede the use of the structure.

Fiber optic sensors are ideal for long term health monitoring of a structure [4]. An extrinsic Fabry-Perot fiber optic sensor measures the phase difference between two reflective surfaces; this phase difference can then be used to determine the strain. Fiber optic sensors can be embedded within the structure itself, or even bonded to the surface of a structure. In addition, optic sensors do not require conventional wiring as in the case of strain gages and LVDT's.

Research in smart structural systems using fiber optic sensors has developed from investigations in other areas. Embedded fiber optic sensors have been successfully used in the manufacture of filament wound pressure vessels, as described by Chang, Foediger, Sirkis, and Vandiver [5]. It was observed in their research that the embedded Bragg grating sensors accurately measured the strain at the location of the sensor. The successful implementation of fiber optic sensors has allowed other researchers to expand on the concept by applying this technology in innovative ways. Krishnamoorthy [6] fabricated

hybrid FRP rebars with embedded fiber optic sensors for use in concrete structures. From the tensile testing of smart hybrid FRP rebars, it was observed that the embedded fiber optic sensors could determine the strain within the rebar. Sutinjo [7] provides a comprehensive analysis of the extrinsic Fabry-Perot interferometric (EFPI) fiber optic sensors used in [6]. This research has monumental significance in that real time sensing of a concrete structure can be performed without using traditional sensing equipment. Furthermore, sensing of the structure will occur for the life of the structure, since the sensors are protected by the elements.

C. RESEARCH OBJECTIVE AND PROBLEM DEFINITION

While more and more structural engineers are accepting FRP as a viable structural component, an effort must be made by the research community to expedite the use of FRP as much as possible. As a result, research to develop a FRP reinforcing with ductility and stiffness characteristics comparable to that of steel reinforcing is the ultimate goal. The research presented in this report will concentrate on manufacture of a final commercial FRP rebar product featuring pseudo-ductility, and the evaluation of its performance in bare conditions as well as inside concrete beams. Tensile testing of the proposed hybrid FRP rebars will be performed, as well as monotonic and repeated loading tests on hybrid FRP reinforced concrete beams. In addition, the added benefit of structural health monitoring using fiber optic sensors embedded in the FRP will be emphasized and will definitely accelerate the use of such a FRP as an alternative to steel in the future.

One possible solution to the lack of ductility in current FRP is a hybrid composite system [6]. The proposed hybrid system consists of varying types of fibers which fail at different times during the load history of the reinforcing. In addition to using a variety of fibers, different manufacturing techniques can be applied to help increase ductility. This research paper presents the findings of tensile tests performed on various hybrid FRP reinforcement, as well as flexural tests on hybrid FRP reinforced concrete beams.

D. REPORT OUTLINE

This report consists of seven sections. Section I contains a brief introduction of FRP and its various applications to civil engineering. Issues concerning ductility will be introduced as well as deficiencies in currently available FRP rebars. Past research on FRP in civil engineering is presented in Section II. Examples of various manufacturing techniques, past research on hybrid FRP rebars, flexural testing of FRP, bond issues, and health monitoring research will be summarized. Section III explains the manufacturing process of the proposed hybrid FRP reinforcing, as well as fiber optic sensor implementation. A detailed explanation of the proposed manufacturing process is given. Sections IV and V present results and discussions on FRP rebar testing and reinforced concrete beam testing, respectively, including the results of fiber optic sensors. After determining the engineering properties of the proposed hybrid FRP through extensive tensile coupon testing, flexural testing of hybrid FRP reinforced concrete beams will be presented. Section VI presents the results of bond tests. Finally, Section VII provides conclusions on this research and recommendations for future research in the area of pseudo-ductile hybrid FRP rebars.

II. LITERATURE REVIEW

A. GENERAL

Research in the area of FRP rebars has developed rapidly. Most research has been focused on bond characteristics of FRP rebars, structural behavior of FRP reinforced and prestressed concrete members, and structural design methods of FRP reinforced concrete structures. Since current FRP rebars lack ductility, research in the development of a ductile FRP rebar has sparked new interest within the research community. Past research on the topic of hybrid FRP rebars address many different areas. These areas include manufacturing techniques for FRP rebar, hybrid FRP reinforcing systems, flexural and shear testing of FRP composites, bond characteristics of various FRP rods, and fiber optic sensor embedment within FRP composites.

B. FRP MANUFACTURING TECHNIQUES AND HYBRID FRP SYSTEMS

Due to the multiple manufacturing techniques available to FRP many different approaches have been developed. The most common manufacturing techniques for FRP rebars are the pultrusion technique, filament winding, and braiding. Tamuzs and Tepfers [8] tested two different types of hybrid FRP rebars. The first type consisted of multiple fibers embedded in an epoxy resin matrix. The manufacturing process for the first type of hybrid FRP rebars was not specified in [6]. Their proposed concept was to achieve ductility by selecting fibers that would fail at different strains causing a gradual failure of the hybrid FRP. An attempt was made to randomly mix the various fibers over the cross section, however this was not possible due to various fiber sizes. These first efforts failed, since high stress concentrations at the location of fiber breakage damaged the

surrounding fibers. It was concluded that the high stress concentrations were a result of the inability to randomly distribute fibers over the cross section. Their second attempt at a ductile FRP rebar consisted of braided FRP rebars with different core materials. As tension was applied the braided FRP shell compressed the core material, thus causing a reorientation of the braided fibers. The reorientation of fibers resulted in large deformations in the braided FRP rebar, but the cross section was reduced due to the compression of the core material.

Bakis, Nanni, and Terosky [9] also performed research on pseudo-ductile pultruded FRP rods. Rods using between two and three different fibers were designed using the rule of mixtures. These rods were then tested under tension, and the desired pseudo-ductile behavior was observed. However, premature failure of the hybrid rods occurred due to the same local stress concentrations observed by Tamuzs and Tepfers.

Belarbi et al., [4] based their research on a hybrid system, but incorporated multiple manufacturing steps to further increase ductility in their proposed hybrid FRP rebars. Belarbi et al., proposed an inner core of various stiff carbon fibers fabricated using the pultrusion process; this hybrid rebar was first proposed in 1995. The behavior of the core would follow the rule of mixtures, assuming randomly distributed fibers in the core. Then, a second manufacturing step was then introduced based on the findings in [6]. The inner core was placed in a filament winding machine and wound with additional fibers. Under tension, it was theorized that the filament wound fibers would reorient themselves after rupture of the core. This reorientation would provide additional ductility as was observed in [6]. To further research in this area, the Composite Manufacturing

Laboratory at the University of Missouri - Rolla was expanded to include a pultrusion machine and a filament winding machine.

Most recently, a second generation ductile hybrid rebar was developed and extensively tested by Harris, Somboonsong, Ko, and Huesgen [10]. Their manufacturing process also included two steps; braiding of various fibers was performed before the final pultrusion process cured the matrix. Their proposed system included stiff fibers located in the center of the rebar, with various aramid fibers braided around the stiff center fibers. Braiding of the fibers was performed to provide some ductility to the rebar as well as to provide bond to the surrounding concrete. Small scale concrete beams were formed using the second generation hybrid rebars, and pseudo-ductile behavior was observed. Furthermore, repeated loading tests were performed on the test beams, with comparisons made to steel reinforced beams. They concluded that the second generation hybrid FRP rebars could provide adequate ductility and bond when compared to steel rebars.

Research in the actual manufacturing technique of FRP rebars is also important, since optimization of the manufacturing process of FRP rebars would reduce the cost of FRP reinforcing. Jiang [11] performed heat transfer analysis that occurs during the pultrusion process. Based on his analysis, his conclusions provide an optimum pulling speed for a given pultruded FRP composite.

C. TESTING OF FRP REINFORCING EMBEDDED IN CONCRETE

To understand the necessity for a gradually failing hybrid FRP reinforcing, past research on conventional FRP reinforcing should be evaluated. Hamid, Saboni, and Mokhtar [12] performed flexural testing on one way concrete slabs reinforced with glass

FRP (GFRP) bars. For comparison, flexural testing was also performed on similarly designed one way concrete slabs reinforced with conventional mild steel rebars. From their experimental testing program, the deflection of the GFRP reinforced beam was always greater than the steel reinforced beam at a given capacity. From their research, an obvious conclusion can be made in that ACI service load deflection provisions may control the design of a GFRP reinforced slab, and more reinforcing than necessary may be required to decrease service load deflections. Furthermore, brittle failure in all GFRP slabs was exhibited, due to the lack of ductility of GFRP. It was determined [12] that rupture of the GFRP rebars can be avoided if a larger percentage of reinforcing is used as compared to the similarly designed steel reinforced slab.

Another application of FRP composites in civil engineering is in prestressed concrete. FRP composites exhibit high stiffness at extremely high stress levels. Prestressed concrete demands high tensile stresses from reinforcing as compared to reinforced concrete where the tensile stresses are typically four times less. Thus, research in this area has been quite promising, and some field applications have already been in service for over ten years. Taerwe and Matthys [13] performed research on concrete slabs prestressed with carbon FRP tendons, Arapee FRP tendons, and conventional steel tendons. Comparisons between load deflection curves of CFRP, Arapee, and steel tendons indicate comparable stiffnesses and deflections until failure. In addition, tests on partially prestressed slabs (Arapee prestressed tendons with CFRP non-prestressed reinforcement) was also performed. The results of these tests prove the hybrid concept has merit since the partially prestressed slab exhibited the best behavior in terms of load and deflection.

Other researchers have abandoned the concept of internal hybrid rebars in lieu of separate embedded composite reinforcing. The research of Razaqpur and Ali [14] is quite notable in this respect. Inverted T beams were poured with two different types of reinforcing; plain carbon fiber rods were used to provide initial stiffness during service load conditions, while a high density polypropylene (HDPP) was used to provide ductility after rupture of the carbon fiber rods. From the test result, it was observed that ductile behavior was achieved from the separate embedded composite reinforcing. However, a sudden drop in load occurred after rupture of the carbon fiber rods. Efforts to reduce or eliminate this drop in load must be performed for this reinforcing concept to be accepted as a viable alternative to steel reinforcing.

D. FRP REBAR BOND RESEARCH

Many papers have been published on the topic of FRP rebar-concrete bond interface. This bond interface is required to transfer stresses from the concrete to the steel. Possibly the most comprehensive analysis of FRP rebar bond testing is presented by Cosenza, Manfredi, and Realfonzo [15]. Many different mechanics of stress transfer are summarized in [15] including chemical bond, friction between the FRP and concrete, mechanical interlock, and hydrostatic pressure due to shrinkage of concrete. Since steel rebars use mechanical interlock as the main stress transfer mechanism, efforts to reproduce mechanical interlock in FRP rebar have been attempted using the filament winding technique or molding of deformations. The objective of mechanical interlock is to crush the surrounding concrete or to yield the deformations; this would lead to a gradual pullout of the reinforcing. Some researchers consider a gradual pullout of

reinforcing related to the ductility issue; thus their focus was ductility in FRP rebars due to successive failure of rib deformations. Using the filament winding technique, a single fiber is placed on the surface of the rebar in a spiral pattern to act as ribbing or deformations. However, from the tests summarized in [15], it was observed that no mechanical interlock was created by the spirally placed fiber. In addition, molding of deformations on the surface of the FRP rebar do not provide adequate mechanical interlock, since it has been observed in [15] that the moldings tend to shear off at the surface of the rebar.

Since the integration of mechanical interlock does not adequately provide bond, other alternatives have been researched. One simple but effective technique to increase the frictional bond between FRP rebars and concrete is to produce an extremely rough surface coating on the FRP rebars. The most common technique for this is the grain covered outer surface, as discussed in [13]. By grain covering the surface of FRP, a frictional value exceeding that of steel has been experimentally observed. The only drawback to this alternative is the relatively sudden pullout that occurs after the frictional bond is broken.

E. PAST RESEARCH ON FIBER OPTIC SENSOR IMPLEMENTATION

Research in smart structural systems using fiber optic sensors has developed from investigations in other areas. Embedded fiber optic sensors have been successfully used in the manufacture of filament wound pressure vessels, as described by Chang, Foediger, Sirkis, and Vandiver [16]. It was observed in their research that the embedded Bragg grating sensors accurately measured the strain at the location of the sensor. The

successful implementation of fiber optic sensors in pressure vessels [16] has allowed other researchers to expand on the concept by applying this technology in innovative ways. Krishnamoorthy [6] fabricated hybrid FRP rebars with embedded fiber optic sensors for use in concrete structures. From the tensile testing of smart hybrid FRP rebars, it was observed that the embedded fiber optic sensors could determine the strain within the rebar. Sutinjo [7] provides a comprehensive analysis of extrinsic Fabry-Perot interferometric (EFPI) fiber optic sensors embedded in composite bars. This research has monumental significance in that real time sensing of a concrete structure can be performed without using traditional sensing equipment. Furthermore, sensing of the structure will occur for the life of the structure, since the sensors are protected by the elements.

F. FUTURE DIRECTION OF FRP RESEARCH

The recent developments in FRP discussed above are an excellent foundation for future research. The research summarized is only a representative sample of hundreds of conclusions. One common conclusion many researchers have observed is the lack of ductility in current FRP rebar technology. As a result, future research in FRP will be focused on addressing issues which will accelerate the use of FRP in field applications. Ductility in FRP rebars and health monitoring capability are two such research areas which will enhance the usage of FRP in the future.

III. FABRICATION OF SMART HYBRID FRP REBARS

A. GENERAL

In order to fabricate a suitable replacement for steel using FRP, the concept of reinforced concrete must be understood. Concrete is a non-homogeneous material which possesses interesting engineering properties. If designed properly, plain concrete can withstand up to 20,000 psi in compression. However, this same concrete would only be able to carry 700 psi in tension. For each square inch of concrete in compression, 28 square inches of concrete in tension would be required to maintain equilibrium of tensile and compressive forces. Furthermore, a plain concrete structure would not give any warning if collapse was evident. For these reasons, a plain concrete structure is not feasible. To account for the deficiency of tensile strength in concrete and to provide warning before failure, mild steel is used in reinforced concrete. The tensile forces developed in steel can easily counteract the compressive forces in concrete, and an efficient and safe structure can be designed.

Reinforced concrete structures are designed to be under-reinforced, meaning that as the two materials work together during the load history of the structure, the steel reinforcing always reaches its tensile yield point before the concrete begins to fail in compression. The requirement of an under-reinforced concrete structure implies there is an optimum ratio between the area of steel and the area of concrete in a given cross section. As load is applied to a concrete structure, stresses develop in both the steel and concrete following their individual stress strain relationships. In an under-reinforced case, the peak concrete compressive stress is reached when the steel is already in the

yielding region, allowing large gradual deformations which are easily noticeable. If this optimum ratio is exceeded or the reinforcement has no yielding plateau, the concrete will fail in compression before the steel can yield; the end result is a brittle failure mode. Linear elastic FRP rebars exhibit a brittle failure mode in concrete; either concrete crushes or the rebar ruptures; both usually occur without warning. Thus, one criterion for hybrid FRP reinforcing is the need for a comparable pseudo-yield stress with mild steel reinforcing.

A second criterion for FRP reinforcing is its stiffness as compared to mild steel reinforcing. Stiffness in reinforced concrete is required to minimize service load deflections. While many types of carbon fibers meet or exceed the stiffness requirement alone, the volume fraction of the composite coupled with the failure strain of the fiber dictate the stiffness of the FRP reinforcing. The volume fraction of any composite is defined as the relative proportions of fibers to matrix material [2] by cross sectional area, volume, or weight. Since most carbon fibers cannot reach their failure strain at a stress comparable to mild steel reinforcing as seen in Figure 1, the result is always a lower stiffness as compared to steel.

Finally, the ultimate failure strain of any non-prestressed reinforcing should be quite large with respect to the concrete crushing strain. This requirement allows excessive deformations to occur, as explained above. For any FRP reinforcing, the ultimate failure strain will correspond with the largest failure strain of the fibers in the composite, unless some rearrangement of the fibers occur during the load history. For example, if a FRP rebar consisted of fibers oriented at an angle with respect to the longitudinal axis of the rebar (in the case of braiding and filament winding), these fibers

would tend to realign themselves with the longitudinal axis as tension was applied. Such rearrangement has been observed to provide additional ductility by physically increasing the length of the rebar [6].

Fiber reinforced composites consist of fibers embedded in a matrix material. The matrix binds the fibers together, transfers loads to the fibers, and protects the fibers. The mechanical properties can be controlled through selection of the fiber and matrix materials, the relative proportion of fiber to matrix (expressed as fiber volume fraction mentioned earlier), the fiber orientation, and fabrication method. The stress strain behavior of composites is a combination of the fiber and matrix properties and is intermediate to that of the fiber alone and the matrix alone [2]. Figures 1 and 2 show the typical stress strain curves of fibers and matrix resins, respectively. Another major advantage of fiber composites is their corrosion resistance. When compared to steel, fiber composites will last longer and thus reduce repair and replacement costs. Finally, when electromagnetic immunity is required, fiber composites are the material of choice.

B. THEORETICAL INVESTIGATION

Based on the theoretical and experimental findings of Krishnamoorthy [6], a theoretical investigation using the concept of hybrid FRP was defined. The concept of a hybrid FRP rebar is based on the utilization of several types of fibers used simultaneously within the composite. Fibers of various stiffness are desired to enhance the overall ductility of the composite. As tension is applied, the fiber with the lowest failure strain will fail first; this point is considered the pseudo-yield point. The sequential failure of the other fibers in order of increasing failure strain will produce the desired pseudo-ductility

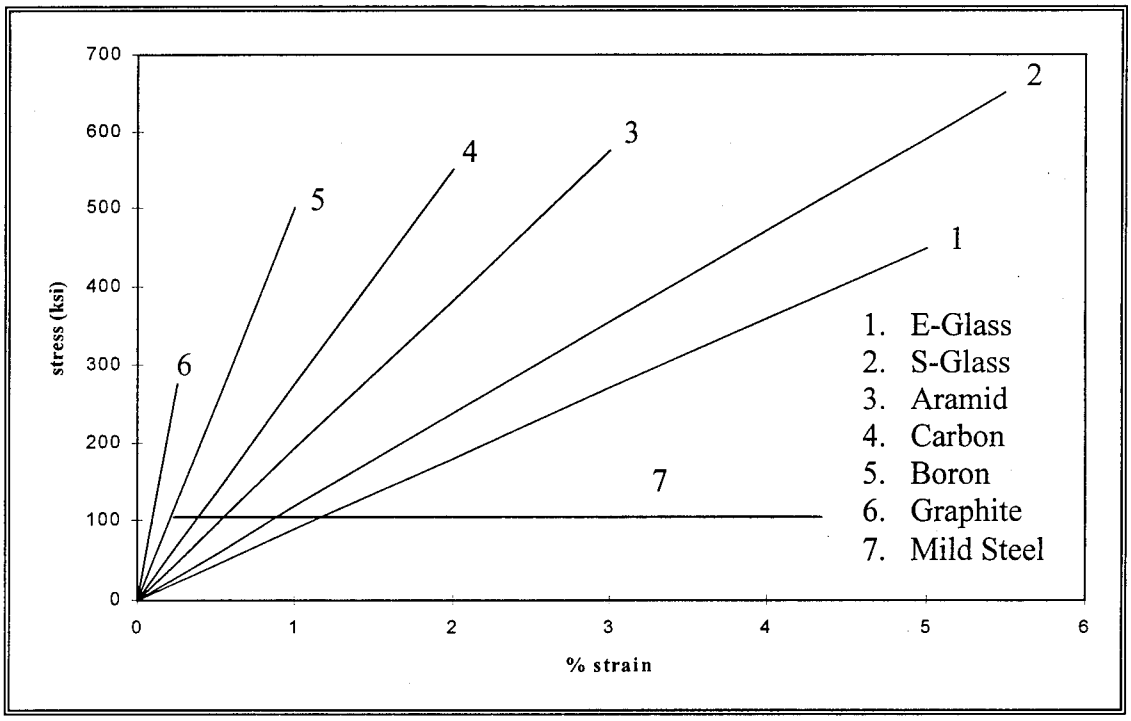

Figure 1 Typical Stress Strain Curves for Fibers and Mild Steel

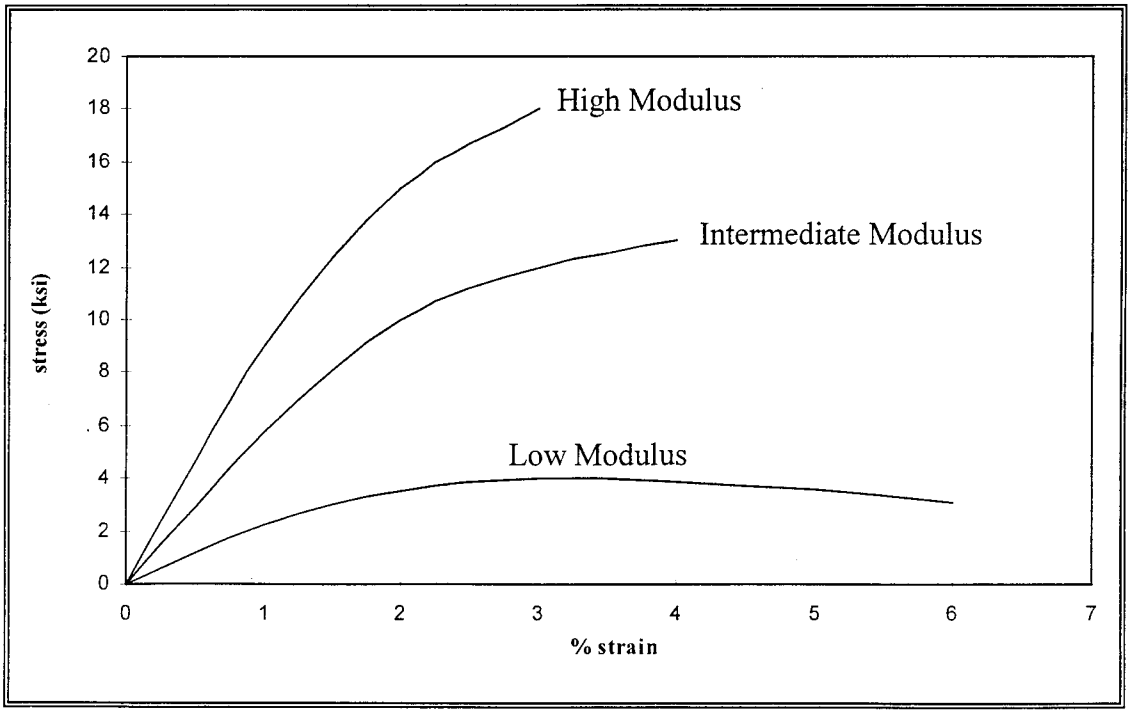

Figure 2 Typical Stress Strain Curves for Matrix Resins

for the overall rebar, while maintaining the required strength. Figure 3 is an illustration of a typical hybrid FRP rebar showing various types of fibers.

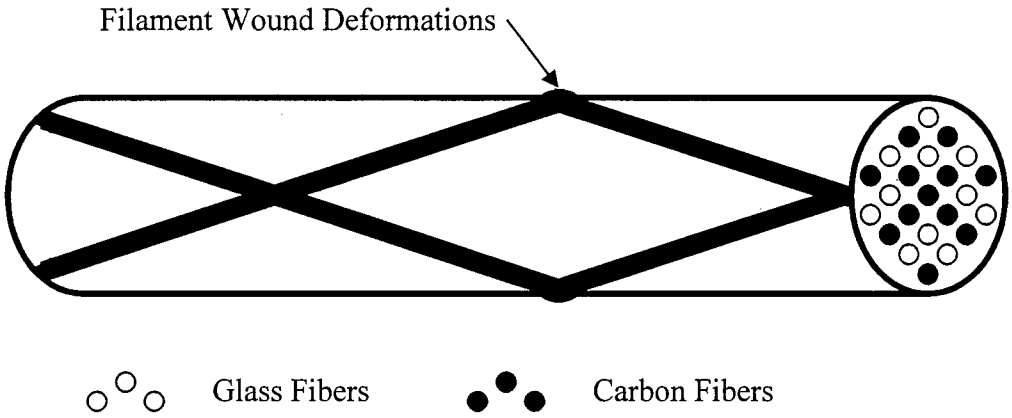

Figure 3 Typical Hybrid FRP Rebar

Unidirectional composite material properties have been shown to follow the rule of mixtures [2]. The mathematical expression for the rule of mixtures is as follows:

$$E_{composite} = E_{matrix}V_{matrix} + \sum_{i=1}^{n} E_{fi}V_{fi} \qquad (1)$$

where E represents the stiffness and V represents the fiber volume fraction. The subscript f represents different fibers in the composite. It is important to note that since most fibers are linear elastic until failure, this expression can be modified to represent the stress of the composite as well. In addition, an assumption is made in that as each fiber reaches its failure strain, that particular fiber does not contribute to the stiffness, nor does it carry

any additional load. After each fiber breaks, the stiffness is re-computed using Equation 2, without the contribution of the broken fiber.

$$E_{composite} = E_{matrix}V_{matrix} + \sum_{i=2}^{n} E_{fi}V_{fi} \qquad (2)$$

To an extent, the rule of mixtures theoretically predicts the material properties of a unidirectional composite. However, upon preliminary testing of glass and carbon hybrid rods designed using the rule of mixtures it was observed that when one fiber breaks, shock waves propagate from the broken fiber to other fibers, causing premature failure in sequential fibers [8,9]. The shock wave is amplified if the fibers are not evenly distributed over the cross section of the composite. Premature failure of fibers translates to an actual composite stress-strain relationship that is always less than the theoretical rule of mixtures stress-strain relationship. One way to prevent premature failure is to disperse the fibers evenly over the cross section of the composite, thus ensuring no eccentric stress redistribution when one fiber breaks. While this may be true, it physically may not be possible due to the manufacturing technique, the tow size, and/or filament diameter of the fibers.

C. PROPOSED HYBRID FRP MANUFACTURE TECHNIQUES

While it may not be possible to evenly distribute fibers over the cross section of a composite, by combining two different manufacturing techniques it is possible to symmetrically distribute different types of fibers over the cross section of a composite. Beginning with the pultrusion technique, a unidirectional core consisting of only one type

of fiber is produced. In the pultrusion technique shown in Figure 4, fibers are first pulled through a resin bath. Once the fibers are impregnated with resin, preformers create the shape of the final product. Finally, the impregnated fibers are pulled through a heated die which cures the matrix and gives the pultruded section its final shape. To allow for different diameter rebars to be fabricated using the same pultrusion machine, two steel plates between the heating elements were designed to accommodate 3/16 inch outside diameter to 3/8 inch outside diameter brass tubing to act as the actual die. The tubing could easily be removed from the steel plates for repair and/or replacement. Most commercially available FRP reinforcing products are produced using the pultrusion technique because of its economic process and minimal fiber waste.

Once the core is produced, a filament winding machine as shown in Figure 5 is used to symmetrically place additional fibers around the core. In this research, a computer controlled three axis filament winding machine was used to wind fibers around the core. A great advantage of any computer controlled filament winding machine is its ability to precisely apply fibers around a mandrel. Since symmetric fiber placement is desired, parameters such as the diameter of the core, the wind angle, and the bandwidth of the fibers used must be entered into the filament winding machine prior to winding. The wind angle is measured from the longitudinal axis of the core to an axis perpendicular to the core. Each fiber has its own bandwidth, or the width of a fiber tow when it is spread across the mandrel. The core is placed in the chucks of the headstock and tailstock axes, and as these two axes rotate in the same direction, a third axis applies fibers to the surface of the core. To achieve longitudinal strength and stiffness as required in FRP reinforcing,

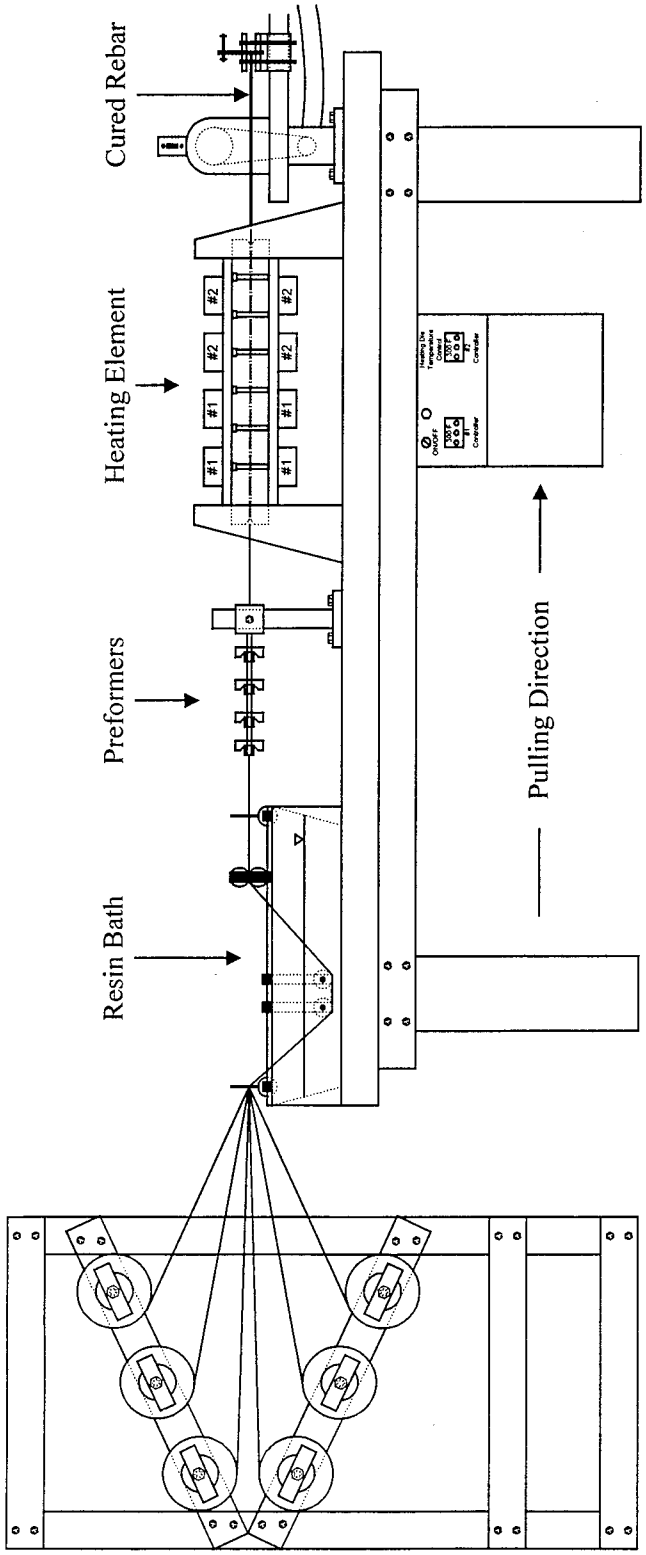

Figure 4 Pultrusion Machine

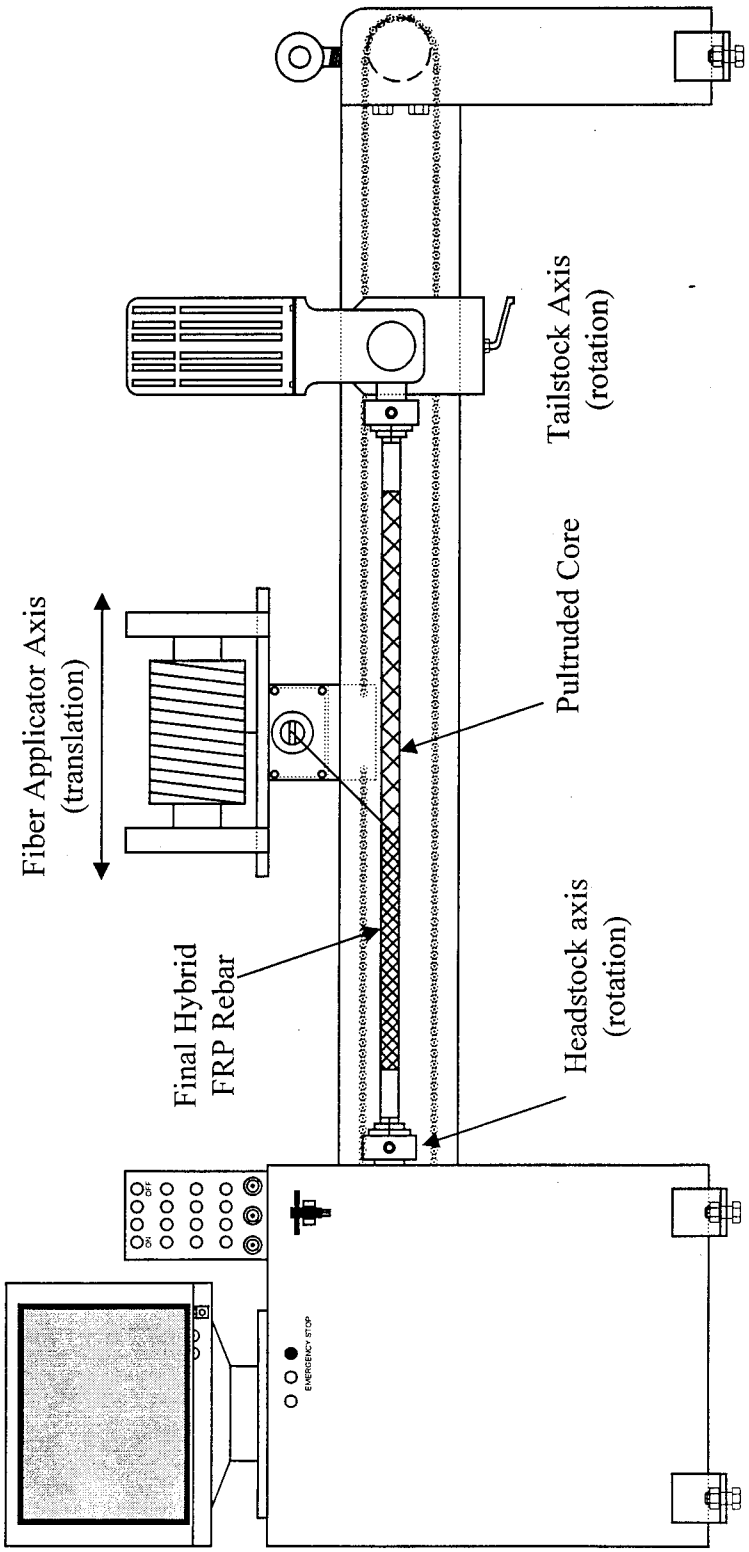

Figure 5 Filament Winding Machine

filament wound fibers were placed with a low wind angle with respect to the longitudinal axis of the core. All filament wound rebars were cured at room temperature for a period of 48 hours.

The final hybrid FRP rebar consists of one type of fiber in the core, with two fibers symmetrically placed on the surface of the core. It is believed that symmetric fiber placement would eliminate any eccentric stress redistribution during fiber breakage.

In order to develop and transfer stresses in a reinforced concrete structure, a bond must exist between the reinforcing and concrete. There are two components of this bond in current mild steel reinforcing; frictional bond and bearing bond. Frictional bond relies on the adhesion of the reinforcing to the concrete. In other words, once the frictional bond is broken, there is no more bond. Developing stresses based on frictional bond alone would require a large rebar embedment length. Conversely, bearing bond is created through a mechanical interlock between the deformations of reinforcing and the surrounding concrete. For a bearing bond to fail, either the concrete must undergo splitting, or the deformations on the reinforcing must yield.

In FRP reinforcing, a conscious effort has been made to improve both the friction and bearing bond [15]. It has been shown that a large frictional component can be developed by simply sand coating FRP reinforcing. However, this frictional component does not provide adequate bond between the reinforcing and concrete. Once the frictional bond is broken, nothing prevents complete pullout of the reinforcing. Thus, a bearing bond must be incorporated into the FRP reinforcing to provide an adequate amount of bond. Many FRP manufacturers use filament winding to include some deformations on the surface of the reinforcing. Many studies have shown that this

method of providing deformations does not split the concrete; rather it shears the deformations off the FRP reinforcing and bearing bond is completely lost [15].

The proposed hybrid FRP rebar can easily be sand coated directly after the filament winding process by applying sand to the uncured matrix. In addition, deformations may also be incorporated to increase the bond characteristics. Shearing of the deformations may be eliminated by adjusting the wind angle and interweaving of the fibers that create the deformations, although this has yet to be proven. Since fibers have excellent longitudinal strength, a low wind angle would prevent shearing of the fibers from the rebar. In addition, if the deformations are built up, i.e., many fiber tows are used to create each deformation; this would give the deformations additional strength against shearing.

D. MATERIAL SELECTION

After using the rule of mixtures to develop a theoretical hybrid FRP stress strain relationship, fibers of different stiffnesses and failure strains were sought. Table I shows the materials selected and their corresponding volume fractions. All material properties for fibers and resin were provided by the manufacturers. Zoltek fibers were used in the core, while Mitsubishi fibers were filament wound around the core at an angle of 20 degrees. The wind angle was selected to provide adequate longitudinal strength. The Shell Epon 9500 resin system was mixed with Shell Epi-Cure Curing Agent 9550 at a ratio of 100 parts resin to 33 parts curing agent by volume. During the pultrusion process, 1 part release agent (MOLD WIZ INT-1846) was added to the matrix to prevent adhesion to the heated die.

To accurately develop a theoretical model, all filament wound fibers were adjusted to account for the wind angle. From the volume fractions in Table I, an initial stiffness of 20.7 Msi at a pseudo-yield strain of 0.003 was established. While the pseudo-yield stress at this point is slightly higher than that of mild steel reinforcing, it was determined that this pseudo-yield point would not be reached due to the shock wave phenomena reported by previous investigators [8,9].

Table I Specifications of Proposed Three-Fiber Hybrid Rebar

Fibers	Type	Volume Fraction %	Elastic Modulus (Msi)	Failure Strain in/in	Wind Angle (degrees)	Manufacture Technique
1	Mitsubishi K137HG	5%	131	0.003	20	Filament Winding
2	Mitsubishi K13710	12.5%	94	0.0045	20	Filament Winding
3	Zoltek Panex-33	19%	33	0.0159	0	Pultrusion
Matrix	Shell Epon 9500	63.50%	0.45	0.113	N/A	N/A

E. INTEGRATION OF FIBER OPTIC SENSORS

To incorporate fiber optic sensors inside the proposed hybrid FRP rebar, an intermediate step between pultrusion and filament winding was added. By securing the fiber optic sensor on the surface of the core, the fiber optic sensor was covered by the filament winding process. Complete coverage of the sensor by the filament wound fibers would protect the sensor from the harsh concrete environment. Furthermore, several fiber optic sensors may be placed within the same hybrid FRP rebar to measure strains in various locations along the structure without degradation of the hybrid FRP material

properties. Extreme care must be taken to ensure a reliable ingress/egress point of the fiber optic line. The fiber optic line can be damaged at this point thus rendering the sensor completely ineffective.

F. LIMITATIONS AND DRAWBACKS

There are some drawbacks to the proposed smart hybrid FRP rebar. The Shell Epon resin system is a thermoset resin; once the resin cures, there is no reshaping of the final product. Any thermoset resin system would prevent standard hooks or stirrups to be fabricated at the jobsite. However, this issue is easily resolved by selecting a thermoplastic resin system. In a thermoplastic resin system, localized reheating of the FRP would soften the matrix, allowing the reinforcement to be shaped.

Another limitation is the size of the filament winding machine. The proposed hybrid FRP rebars were fabricated using a Composite Machines Company filament winding machine with a usable mandrel (or core) length of 78 inches. In the future, if longer hybrid rebars are required a larger filament winding machine will be needed.

IV. FRP REBAR TENSILE TESTS AND RESULTS

A. GENERAL

The purpose of the tensile testing program was to determine if the theoretical investigation could accurately represent the material behavior of the proposed hybrid FRP rebars. From the theoretical investigation, a three fiber hybrid FRP rebar should exhibit three peaks, each peak signifying the rupture of one type of fiber. The results of these tensile tests were used in the design of the hybrid FRP reinforced concrete beams in Section V.

B. PREPARATION OF FRP REBAR COUPONS

Tensile testing was performed on each batch of hybrid FRP rebars to account for variations in the manufacturing process. From each batch, three tensile coupons were selected. A gage length of about 24 inches was chosen to allow for a reliable average strain measurement over the coupon.

Researchers have used various methods to test FRP rebars in tension. Malvar and Bish [16] provide a comprehensive overview of various gripping mechanisms. From their research, it was observed that the ASTM standard test method for tensile determination of FRP rebars produced the lowest strength values. In addition, failure at the grip/coupon interface usually resulted in lower strength values. It was determined that a clamp type grip with end wrapped specimens yielded the best results. The testing method and specimen preparation for the testing program was based on the results of [17].

Preliminary tensile testing of the proposed hybrid rebars revealed possible premature failure at the grip/coupon interface. In all preliminary testing, failure of the coupon occurred within the hydraulic grips. It was determined that the serrated edges of the grips crushed the ends of the coupon, thus causing a weak point in the coupon. This phenomenon does not occur in a steel coupon test because steel is isotropic and has equivalent strength in all directions. Furthermore, slippage between the grips and the coupon was also evident in some trial testing. To avoid premature failure at the grip/coupon interface, both ends of each coupon were filament wound with additional carbon fiber to a thickness of twice the rebar diameter. In addition, a hydraulic grip pressure was determined through a trial and error approach to eliminate crushing of the coupon. During some coupon tests, slippage sometimes occurred between the coupon and the filament wound wrap. This slippage was determined by inspecting the ends of the coupons after the test. If substantial slippage had occurred, results from that test were discarded and new coupons were prepared.

C. TESTING APPARATUS AND DATA ACQUISITION

All tensile testing of the proposed hybrid FRP was performed using a MTS Series 880 Universal Testing Machine. This machine uses hydraulic "V" notch type grips with serrated surfaces to test circular cross section specimens. A hydraulic grip pressure of 500 psi was selected to prevent crushing of the coupon while eliminating slippage between the grips and the filament wound ends of the coupon.

To determine the exact load deflection behavior of the proposed hybrid FRP, each tensile test was performed under displacement control at a rate of 0.039 in/minute. A

slow rate was selected to ensure all data collection during the test. For comparison, ASTM D3916-94 (Standard Test Method for Tensile Properties of Pultruded Glass-Fiber-Reinforced Plastic Rod) requires a crosshead speed rate of 0.2 in/minute for a displacement controlled tensile test. The applied load was measured using an internal load cell, while the crosshead motion was monitored by an internal linear variable differential transformer (LVDT). As mentioned in the previous section, after each test the coupon was checked for slippage in the grips. Observation of ends of the coupons would easily determine if slippage had occurred. If any slippage had occurred, the test data was discarded and a new coupon was tested. The test data was collected using a proprietary data acquisition program at a rate of 10 data points per second.

D. RESULTS OF TENSILE TESTS AND DISCUSSIONS

The primary objective of the tensile testing program was to determine if the theoretical stress-strain curve of a hybrid composite rebar could be reproduced through experimental testing. Figure 6 shows the theoretical stress strain curves based on the fiber volume fractions in Table I. There are three distinct peaks in Figure 6; each peak corresponds with the failure of one type of fiber. From the selected materials and volume fractions, this stress strain curve should theoretically provide gradual failure, or in other words the desired pseudo-ductility. The theoretical pseudo-yield point of this hybrid reinforcing occurs at a stress of 62,000 psi, with a pseudo-yield strain of 0.3 %.

Figure 7 compares the theoretical stress - strain curve with the experimental stress strain curve for a typical tensile test coupon fabricated following Table I. From the experimental stress strain results of three tests, an average stiffness of 13.8 Msi was

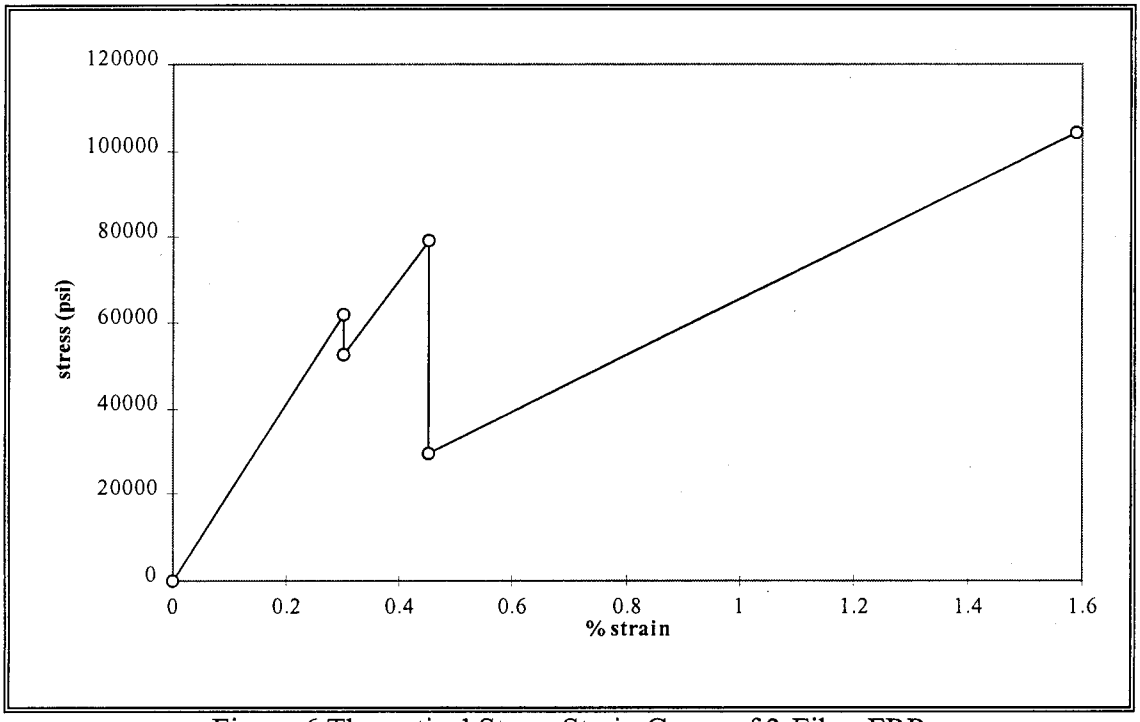

Figure 6 Theoretical Stress Strain Curve of 3-Fiber FRP

computed. The measured pseudo-yield stress was 56,600 psi, while the measured pseudo-yield strain was 0.41%. Under tension, the rebar coupons experienced successive cracking of the filament wound shell. Each crack corresponded with a drop in load, as shown in Figure 6. Furthermore, these cracks were spread out evenly across the gage length of the coupon at a crack spacing of 4 to 5 inches. Figure 8 represents a typical cracking sequence for the coupons tested. It was also observed that the load increased after the occurrence of each crack. Finally, the core ruptured at a strain comparable to that of the Zoltek carbon fibers used in the core.

It is shown in Figure 7 that the experimental stress - strain relationship does not correlate with the theoretical curve. In the experimental curves, five peaks occur during the load history of the coupon using only three different types of fibers. According to the

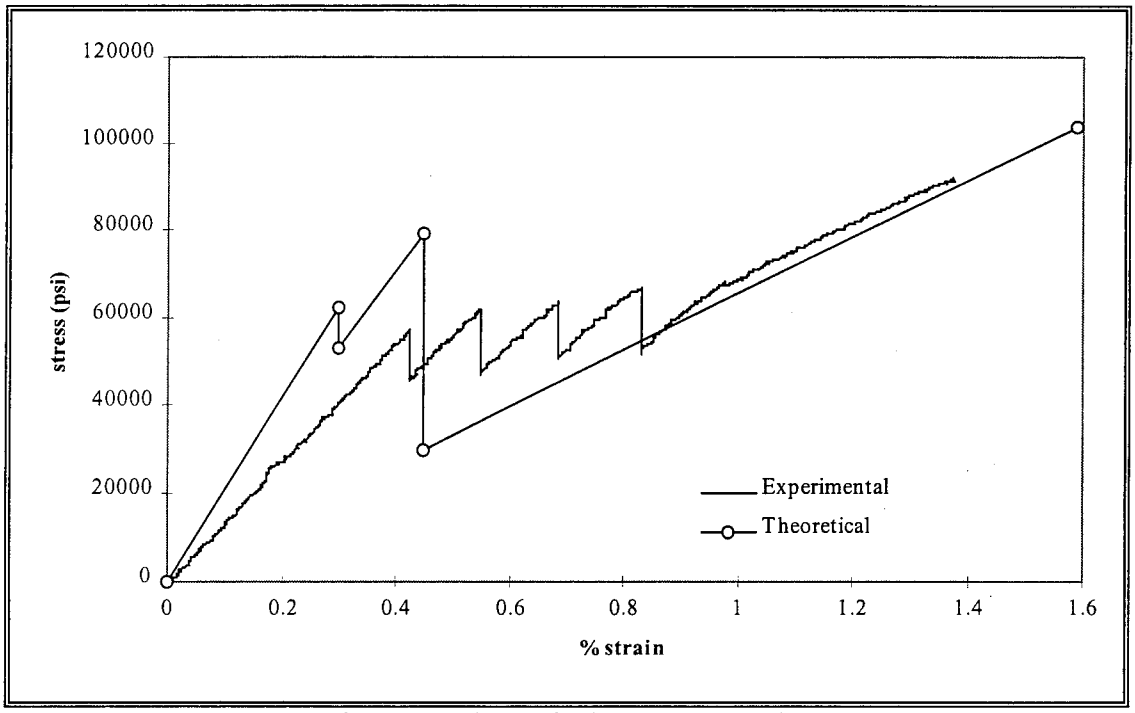

Figure 7 Theoretical vs. Test Results

rule of mixtures, only three peaks should be observed. The difference in behavior can be explained using the analogy of "concrete stiffening," where the shell is the equivalent surrounding concrete and the core is equivalent to steel reinforcing [18].

1. Concrete Stiffening as Applied to Hybrid FRP Rebars. The behavior of the proposed hybrid FRP will be extrapolated from the following explanation of concrete stiffening. A steel bar embedded in concrete is shown in Figure 9. A tensile force is applied to the embedded rebar, and cracking of the concrete will occur. The stress in the rebar at the location of any crack will be higher than the stress in the rebar between two cracks. This phenomenon occurs because the bond between the concrete and steel is still evident, and both materials work together to carry the load between two cracks. In

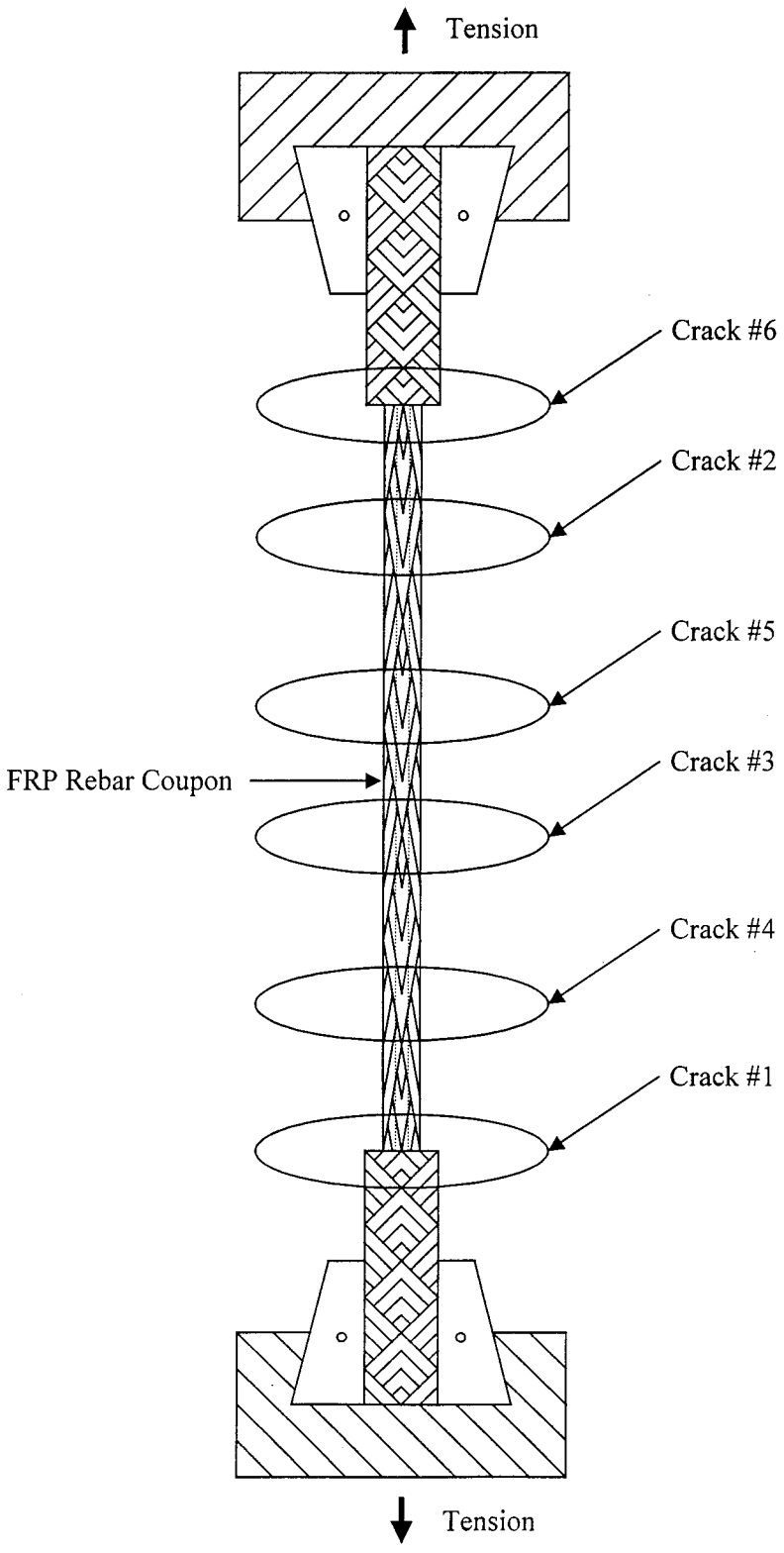

Figure 8 Typical Cracking Pattern for Hybrid FRP Coupon Test

contrast, the bond at a crack is broken, and thus the steel rebar only carries the load. Diagrams of the stresses and strains in steel and concrete between two cracks are also included in Figure 9. From Figure 9, it is shown that the concrete strain at a crack is zero, while the steel strain at a crack is at a maximum. Again, the strains between two cracks are the same for each material, since bond is intact.

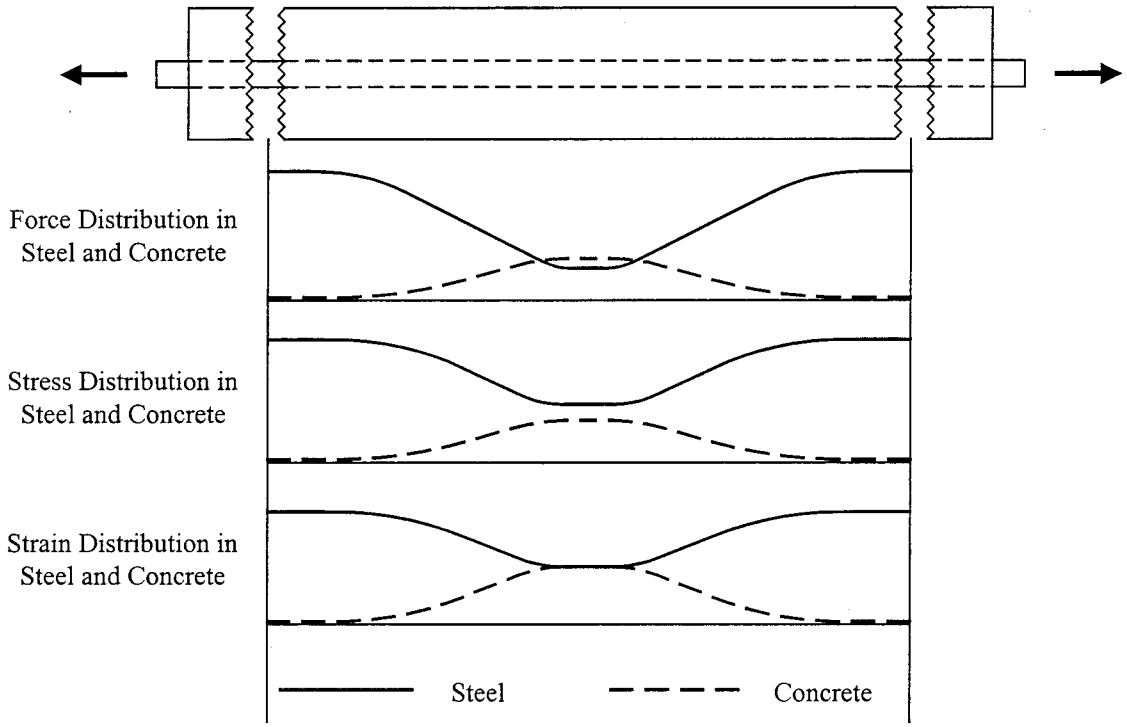

Figure 9 Distribution of Stresses and Strains Between Two Cracks

The very same phenomena summarized above was observed during the hybrid FRP coupon tests. While it is assumed that the stress of the shell is zero at a crack location, some stresses in the shell existed between two cracks. Since the ultimate strains of the materials involved are different, shearing between the different materials is not

negligible, as assumed in the rule of mixtures. In addition, since there were two different filament wound fibers with two different failure strains, composite action between the two different filament wound fibers also existed. For this reason, the pseudo-yield strain did not correlate with either of the failure strains of the filament wound fibers. All successive cracking of the shell occurred at points of weak bond between the shell and the core along the entire rebar, similar to the concrete stiffening concept. It is believed this bond is required to maintain the shearing forces developed between the shell and the core.

The experimental results correlate relatively well at the ultimate peak location of the theoretical stress strain curves, as seen in Figure 7. This correlation occurs in both the theory and the experimental results because the ultimate load is carried by only one type of fiber.

2. Investigation of Two-Fiber Hybrid FRP Rebars. To further understand the behavior of hybrid FRP rebar under uniaxial tension, hybrid rebars with two different fibers were investigated. The materials used and corresponding fiber volume fractions are listed in Table II.

Table II Volume Fractions for Two-Fiber Hybrid Rebars

Fibers	Type	Volume Fraction %	Elastic Modulus (Msi)	Failure Strain in/in	Wind Angle (degrees)	Manufacture Technique
1	Mitsubishi K137HG	15%	131	0.003	20	Filament Winding
2	Zoltek Panex-33	23%	33	0.0159	0	Pultrusion
Matrix	Shell Epon 9500	62%	0.45	0.113	N/A	N/A

The same manufacturing process was used for these hybrid rebars: Zoltek fibers were used in the pultrusion process, while Mitsubishi K137HG fibers were wound around the core. Figure 10 shows the experimental stress - strain behavior of the two-fiber hybrid rebar. Under tension, multiple cracking of the shell was again observed, with a crack spacing between 2 to 3 inches. It is believed the crack spacing was smaller due to the lower failure strain of the filament wound shell. A total of seven cracks were observed during the test. However, some cracking must have occurred simultaneously because only four peaks are evident from Figure 10. A stiffness of 13.8 Msi was experimentally measured, with a pseudo yield strain of 0.31%. The pseudo yield strain observed corresponds with the failure strain of the Mitsubishi K137HG fibers; this agrees with the concrete stiffening concept. Application of the rule of mixtures would also determine a pseudo yield strain of 0.3%; however, the additional peaks until failure can only be explained with the concrete stiffening analogy mentioned above.

One more observation can be made from the experimental stress-strain relationships of both the two-fiber and three-fiber hybrid rebars. If the slopes of the corresponding peaks are extrapolated to the x-axis as shown in Figure 11, the slopes do not pass through the origin. Pseudo-permanent deformation has occurred in the hybrid rebar, due to the multiple cracks in the shell. Furthermore, if the stiffness of the peaks within the pseudo-ductile region are computed, the stiffness computed would be comparable with the initial stiffness before any cracking has occurred. This implies that if the proposed hybrid rebar was exposed to repeated loading, the hybrid rebar would perform similar to steel, although this is speculation at best since no repeated loading tests were performed. This observation is also contradictory to the assumption of the law

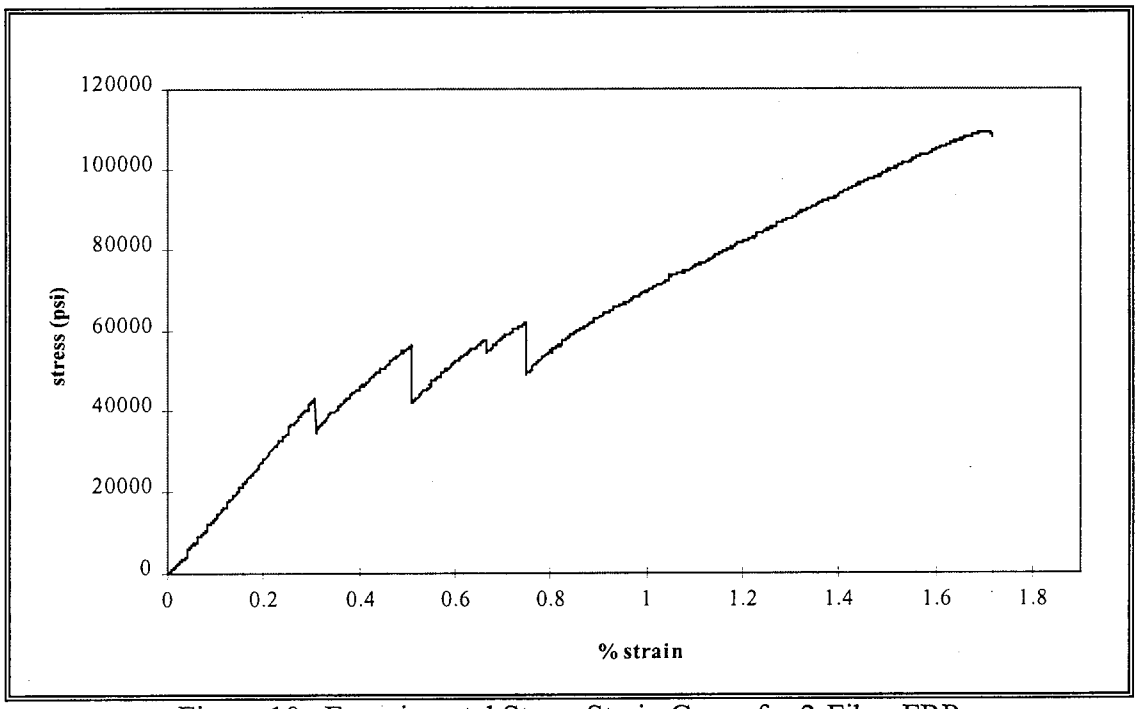

Figure 10 Experimental Stress Strain Curve for 2-Fiber FRP

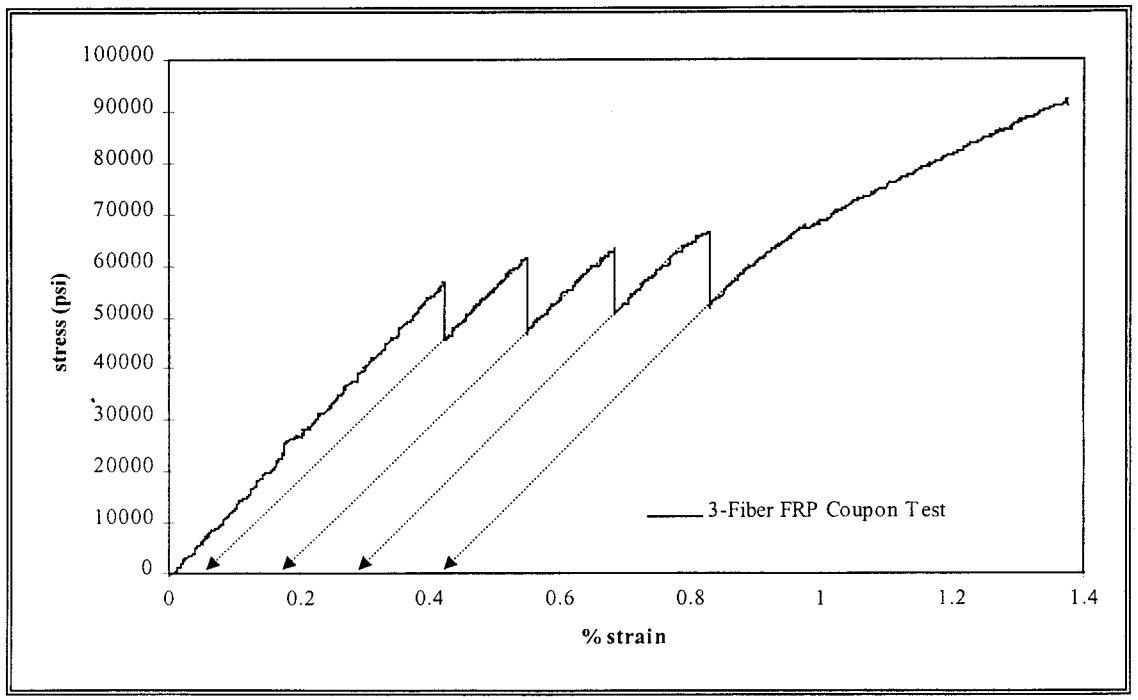

Figure 11 Extrapolation of Peak Slopes in Pseudo-Ductile Region

E. COMPARISON OF HYBRID FRP AND STEEL REINFORCING

of mixtures that residual strains do not exist but stiffnesses reduce after breakage of some fibers.

One of the objectives of this research was to develop a hybrid FRP rebar with comparable engineering properties to that of steel rebar. In this respect, Figure 12 compares the stress-strain curves of the proposed hybrid FRP with conventional Grade 40 and 60 mild steel rebars. Many deficiencies are evident, beginning with the stiffness of the hybrid FRP. The initial stiffness of the hybrid FRP is approximately half when compared to mild steel rebar. This indicates a hybrid FRP reinforced structure will have larger service load deflections as compared to a steel reinforced structure. Another deficiency is the pseudo-yielding plateau of the proposed hybrid FRP. While the small pseudo-yield plateau looks negligible when compared to the steel yielding plateau, this is quite misleading. In some steel reinforced concrete structures, the full yielding region of steel is never fully utilized. Therefore, there is additional ductility that is not used in steel rebar because crushing of the concrete occurs before the strain hardening region is entered. Consequently, the proposed hybrid FRP rebar has adequate pseudo-ductility and a pseudo-strain hardening region for use in reinforced concrete design as shown in the beam test results in Section V.

F. DRAWBACKS IN THE MANUFACTURE OF THE PROPOSED HYBRID FRP

With more experience in the manufacturing techniques of the proposed hybrid FRP system, a suitable corrosion free replacement for mild steel rebars will be possible in the future. From the previous section, three engineering properties require improvement: the initial stiffness, the pseudo-ductile region, and the ultimate strain.

The stiffness of the proposed hybrid FRP system can be improved two different ways. The first solution is to use ultra-high stiff fibers with failure strains comparable to

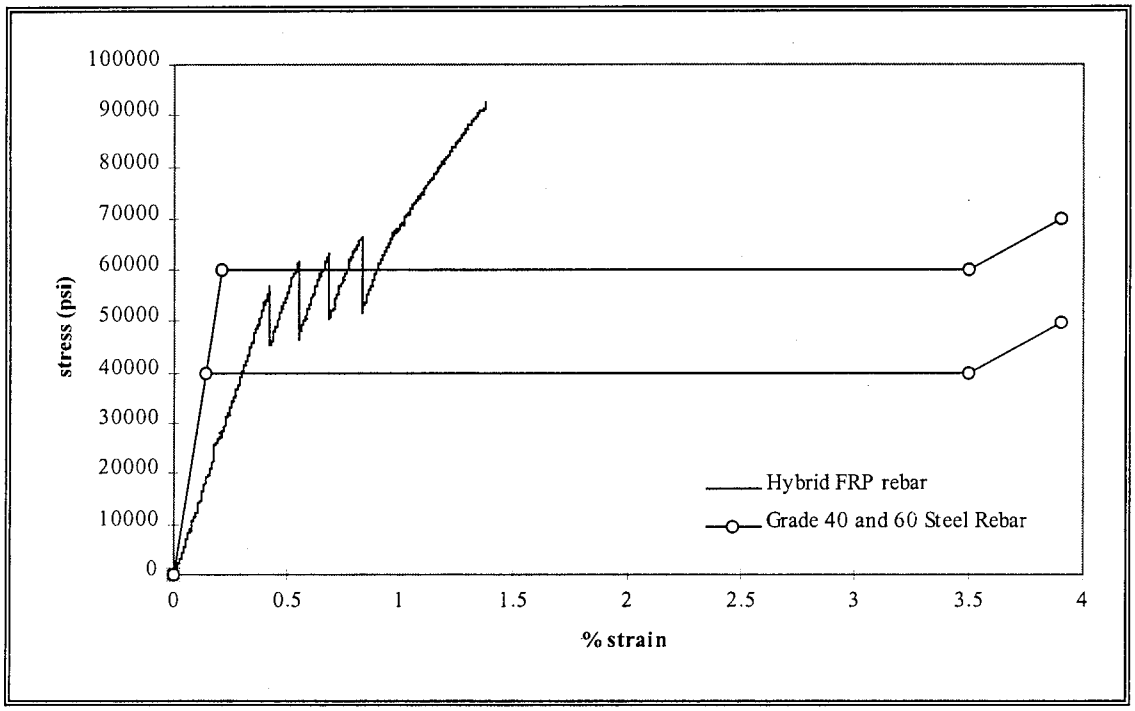

Figure 12 Comparisons Between Hybrid FRP and Grades 40 and 60 Mild Steel Rebars

the yielding strain of steel. These fibers should be used in the filament wound process. By achieving a pseudo-yield strain close to that of steel, the stiffness of the hybrid FRP rebar will approach that of steel. The second solution to increasing the stiffness is to regulate the fiber volume fraction. By increasing the fiber volume fraction, the percentage of load carrying fibers in the cross section is greater, and thus more load will be carried. However, the application of matrix resin in the filament winding process is difficult to control; therefore a desired fiber volume fraction may not be attained. Unless

a custom matrix resin application system is designed for use with the filament winding machine, difficulties will always exist in controlling the fiber volume fraction of any filament wound rebar.

The ultimate strain and pseudo-ductile region are related in that the stiffer the core material is, the smaller the pseudo-ductile region will be. In the future, a hybrid FRP rebar should be fabricated with a pultruded core consisting of a large failure strain fiber such as Kevlar-49, and a filament wound shell consisting of Mitsubishi K137HG. With these fibers, a large pseudo-ductile region and a large failure strain should be observed. Furthermore, the slope of the pseudo-strain hardening region will be reduced thus making it more comparable to the slope of the strain-hardening region in mild steel.

G. CONCLUDING REMARKS

Even though the theoretical investigation does not correlate with the experimental results, pseudo-ductility in the proposed hybrid FRP rebars was achieved. The concrete stiffening concept can be used to explain the experimental results with relative confidence. Furthermore, by placing fibers symmetrically over the cross section of the rebar, eccentric stress redistribution during fiber breakage was eliminated. Additional testing will be carried out in the future to address the issue of slippage at the grip/coupon interface, or mismeasurement of the deformation of the coupon.

There are some shortcomings in the material behavior of the proposed hybrid FRP as well. As mentioned earlier, carbon fibers reach their stiffness at very high stress levels. To achieve a material behavior similar to mild steel reinforcing, the stiffness must be achieved at a relatively low stress. The proposed hybrid FRP reinforcing does not

achieve a stiffness comparable to steel. In addition, the ultimate strain of the proposed hybrid FRP is small as compared to mild steel rebars and the requirements of ASTM A617. With future research and selection of other fiber volume fractions and types, it is believed that the engineering properties of steel can be achieved through the proposed technique.

Further investigation is needed to study the behavior of hybrid FRP rebars in a structural application. A hybrid FRP system with comparable engineering properties to steel will require further research to develop. Yet, it is important to know if the proposed solution to a corrosion free pseudo-ductile rebar merits such future research. The first step in providing a solid foundation to future research in this area is a comprehensive testing program that compares steel reinforcing and current FRP rebar technology with the proposed hybrid FRP rebar system. Section V presents this comprehensive testing program.

V. FLEXURAL TESTING OF R/C BEAMS AND RESULTS

A. GENERAL

To investigate the ductile behavior of the proposed hybrid FRP rebars embedded in concrete, a flexural testing program was performed. The study consisted of six reinforced concrete beams having different types of reinforcement. Two beams consisted of different percentages of steel reinforcing, while three beams were designed with the proposed hybrid FRP rebars. A final beam was designed using unidirectional FRP reinforcing. Monotonic as well as repeated loading tests were performed.

The goal of the flexural testing program was to collect data to compare the behavior of the hybrid FRP reinforced beams with the steel and unidirectional FRP reinforced beams. The comparisons made will help determine if the proposed hybrid FRP system will be a viable corrosion free alternative to steel in the future.

B. THE TEST BEAMS

In order to examine the flexural capacity of a reinforced concrete beam, the overall dimensions of the beam are critical. To accurately test the flexural capacity in a test beam, the shear component should be minimized so that the flexural component can be observed. The shear span to depth ratio of a given beam can provide information to help determine which component dominates the behavior. For example, a beam designed with a shear span to depth ratio less than or equal to 2.5 typically has a large shear component; many different failure modes are observed in the behavior. A testing program should be conceived in such a way that one type of failure mode is forced upon

all the specimens so that comparisons between the different specimens can be made. Thus, a beam designed with a small shear span to depth ratio would not provide representative flexural capacity results. On the other hand, if a shear span to depth ratio between 2.5 and 6 is selected, the shear contribution is not as great, and thus representative flexural capacity results may be obtained.

In this testing program, the overall length of the beams was limited to the length of the hybrid FRP rebars. As mentioned earlier, the proposed hybrid FRP rebars were fabricated using a filament winding machine with a usable mandrel (or core) length of 78 inches. Therefore, the overall length of the test beams was predetermined at 78 inches. Then, to force a flexural failure mode, a shear span to depth ratio greater than 2.5 was selected for a preliminary beam design. A four point bending test was also used to achieve a shear span to depth ratio greater than 2.5 A summary of beam dimensions,

Table III Summary of Beams

Beam	Reinforcing Type	f'c (psi)	Curing Time, days	b (in)	d (in)	A_s (in^2)	ρ
1S1.0	Steel	5500	21	4.75	6.75	0.33	1.0
1FRP1.0	Hybrid FRP	5500	22	4.75	6.75	0.2886	0.9
2FRP1.0R	Hybrid FRP	5500	23	4.75	6.75	0.2886	0.9
2S1.7R	Steel	5500	20	4.75	6.75	0.55	1.7
3FRP1.5	Hybrid FRP	5100	15	4.75	6.75	0.481	1.5
4FRP0.5	Unidirectional	5500	19	4.75	6.75	0.1657	0.5
3S2.0	Steel	4500	28	4.75	6.75	.66	2.0
5FRP1.8	FOS Hybrid FRP	4500	28	4.75	6.75	0.58	1.8
5FRP1.8	FOS Hybrid FRP	4500	28	4.75	6.75	0.58	1.8

concrete strength, and reinforcing percentage is shown in Table III. Beams designated with an "R" signify a repeated loading test, while all other beams underwent monotonic loading until failure. Two beams (5FRP1.8 and 5FRP1.8) were instrumented with fiber optic sensors.

Since the objective of this testing program requires a flexural failure mode in the test beams, all shear reinforcing according to ACI 318-95 was over-designed to prevent any type of shear failure mode. For all test beams, shear reinforcing was fabricated from #3 Grade 40 mild steel reinforcing bars. Figure 13 shows the locations of all shear reinforcing as well as the support and load points.

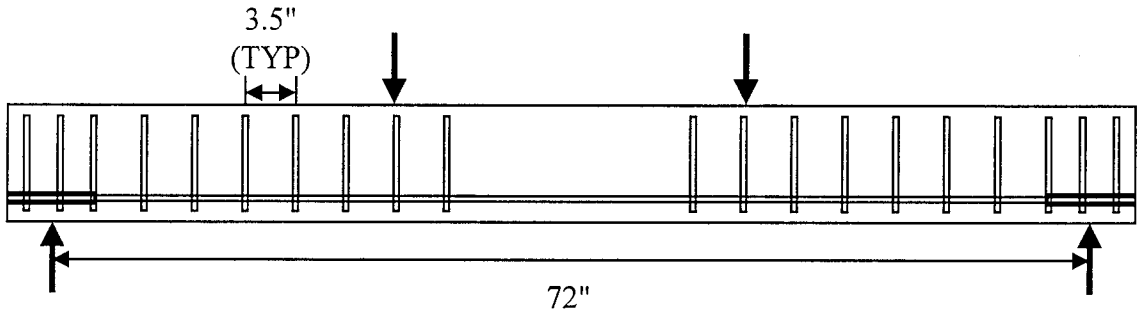

Figure 13 Typical Stirrup Placement

C. MATERIALS

1. Concrete. The concrete used in all the test beams was designed to achieve a 14 day compressive strength of 4000 psi. The material quantities for each batch are shown in Table IV:

Table IV Concrete Mix Design

Type I Portland Cement	558 lb/yd^3
Water	295 lb/yd^3
Fine Aggregate	1400 lb/yd^3
Coarse Aggregate (1/2" M.A.S.)	1410 lb/yd^3
w/c Ratio	0.55
Slump, in	2.75 - 3.75
Density	140 lb/cf

Standard 6 inch by 12 inch concrete cylinders were prepared from each batch of concrete. Cylinders were capped using a sulfur capping compound according to ASTM C617 and tested according to ASTM C39 the day of the beam test.

For design purposes, the stress strain relationship of concrete was taken to follow a parabola:

$$\frac{f_c}{f'_c} = \frac{2\varepsilon_c}{\varepsilon'_c} - \left(\frac{\varepsilon_c}{\varepsilon'_c}\right)^2 \qquad (3)$$

where f_c = concrete compressive strength at ε_c
f'_c = ultimate concrete compressive strength
ε'_c = ultimate concrete compressive strain, taken as 0.003
ε_c = concrete compressive strain

2. Reinforcement. In addition to the concrete stress strain relationship, the stress strain relationships of the three types of reinforcing are also required to develop the most accurate theoretical design. In this study, the tensile stress strain relationships of the various reinforcing used were taken as the following:

For Grade 40 mild steel reinforcing:

$$\begin{aligned} 0 < \varepsilon_s \le 0.002 \quad & f_s = 26150\varepsilon_s \\ 0.002 < \varepsilon_s \le 0.0247 \quad & f_s = 52300 \\ 0.0247 < \varepsilon_s \le 0.0543 \quad & f_s = 41900 + 420\varepsilon_s \end{aligned} \tag{4a}$$

For Hybrid FRP reinforcing:

$$\begin{aligned} 0 < \varepsilon_s \le 0.0041 \quad & f_s = 13800\varepsilon_s \\ 0.0041 < \varepsilon_s \le 0.00827 \quad & f_s = 49200 + 1840\varepsilon_s \\ 0.00827 < \varepsilon_s \le 0.0142 \quad & f_s = 25630 + 4700\varepsilon_s \end{aligned} \tag{4b}$$

For Unidirectional FRP reinforcing:

$$0 < \varepsilon_s \le 0.0159 \qquad f_s = 21900\varepsilon_s \tag{4c}$$

where ε_s = strain in reinforcing (in/in)
f_s = stress in reinforcing (psi)

The above relationships were experimentally determined through tensile coupon testing, except for the unidirectional FRP reinforcing. The rule of mixtures was used to determine the stiffness of the unidirectional FRP reinforcing. For all steel reinforced beams, standard hooks according to ACI 318-95 were fabricated to develop stresses in the longitudinal steel reinforcing. All hybrid FRP reinforced beams used 0.35 inch diameter three-fiber hybrid FRP rebars, while the unidirectional FRP reinforced beams contained 0.1875 inch diameter pultruded rebars. The composite rebars were sand coated to provide some bond as discussed in Section III, however sand coating was not included in the measurement of the rebar diameter. Furthermore, to prevent pullout failure of the composite rebars each end of the rebar was filament wound to a diameter of three times the rebar diameter and sand coated to provide some bearing capacity when embedded in

concrete. All composite rebars were fabricated in the Composite Manufacturing Facility at the University of Missouri - Rolla.

D. DESIGN AND OBJECTIVES OF TESTS

The objective of the testing program was to compare the behavior of different types and percentages of reinforcing under flexure. One method to compare the behavior of different beams is to measure the curvature of each test beam as well as the midspan deflection. Comparisons can then be made between the theoretical approach and experimental test data as well as between different types of reinforced beams.

All beams were designed as under-reinforced beams according to the ultimate strength design approach [18]. In the ultimate strength design approach, a strain compatibility diagram is used to find the relationship between the concrete strain and the reinforcing strain using similar triangles, as shown in Figure 14. If the stress strain relationships of both the concrete and the reinforcing are known, a stress diagram is then produced. Once a stress diagram is established, equilibrium of forces and moments is applied to determine the flexural capacity of the cross section.

To simplify computations and to follow the American Concrete Institute Building Code 318-95, the parabolic compressive stress diagram of concrete was converted to an equivalent stress block using the Whitney's equivalent stress block approach. In the Whitney's stress block approach, the variables α and β_1 are computed to give an equal area when compared to the parabolic stress diagram. Also, the α and β_1 values computed account for the locations of the centroids of both the parabola and the rectangular stress

blocks. Furthermore, the ultimate concrete compressive strain was limited to 0.0035 in/in.

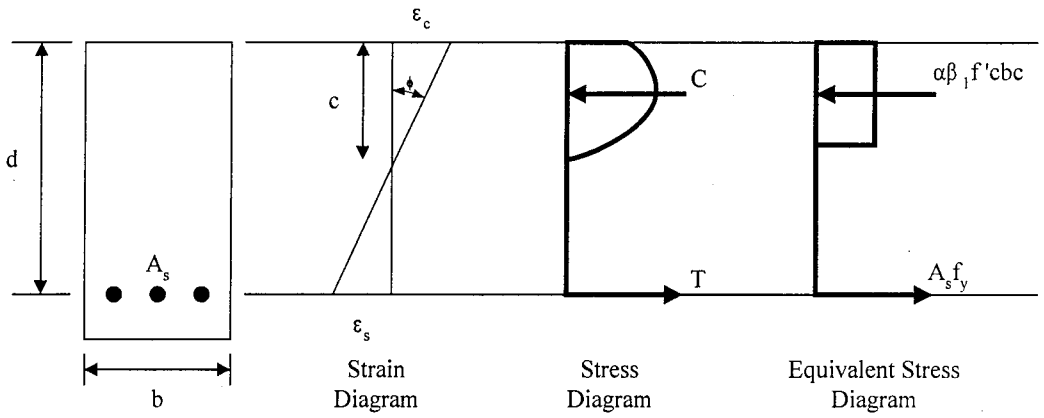

Figure 14 Strain and Stress Diagrams for a Typical Reinforced Concrete Beam

As discussed earlier, an under-reinforced concrete structure implies there is an optimum ratio between the area of reinforcing and the area of concrete in a given cross section. For an under-reinforced beam, this optimum ratio usually called the balanced condition, should never be exceeded. Equation 5 represents the balanced condition for a steel reinforced concrete beam:

$$\rho_b = \frac{0.85\beta_1 f'c}{fy}\left(\frac{87000}{87000+fy}\right) = \frac{A_s}{bd} \qquad (5)$$

where ρ_b represents the balanced condition of concrete crushing at the onset of steel yield. For a steel reinforced beam with a f_y of 52,300 psi and a f'_c of 5,500 psi, a ρ_b of

4.46% is computed. This is a well established equation printed in all reinforced concrete design textbooks.

Since the proposed hybrid FRP rebar does not have engineering properties similar to steel reinforcing, a new equation to determine the balanced condition must be derived so that an under-reinforced hybrid FRP concrete structure can be designed. Equation 6 represents the balanced condition based on the engineering properties of the hybrid FRP rebar:

$$\rho_b = \frac{0.85\beta_1 f'c}{fy}\left(\frac{40500}{40500+fy}\right) = \frac{A_s}{bd} \qquad (6)$$

Using a pseudo-yield stress of 56,500 psi and a concrete stress of 5,500 psi, a ρ_b of 2.76% is computed from Equation 6.

In comparing the percentage reinforcing of each test beam [Table III] with respect to the balanced conditions computed above, all test beams have been designed as under-reinforced beams. Ductile failure should be observed in all test beams with the exception of the unidirectional FRP reinforced beam. Since unidirectional FRP reinforcing has no yield plateau, a brittle failure is expected.

One method to compare the behavior of different reinforced concrete beams is to compute moments and curvatures. To develop moment curvature diagrams for a given cross section, a concrete strain is first selected. From this concrete strain, the corresponding reinforcing strain is determined through the strain compatibility. This step is required to determine if the reinforcing has reached its yield or pseudo-yield point.

Once this has been established, the moment capacity at the given concrete strain is computed by summing moments about the location of the reinforcing:

$$M = \alpha\beta_1 f'_c\, bc\left(d - \frac{\beta_1 c}{2}\right) \qquad (7)$$

In addition, the curvature at the concrete strain must also be computed. The equation for the curvature at a given concrete strain is :

$$\phi = \frac{M}{EI} = \frac{\varepsilon_c}{c} \qquad (8)$$

The curvature represents the reduction of the moment of inertia for a given reinforced concrete cross section. This is an important measure of the ductility of a cross section. Before cracking of the concrete, the moment of inertia is the greatest and the curvature is small since the entire cross section is effective. As tensile cracks begin to occur, the curvature increases due to an increase in the concrete strain and the upward movement of the neutral axis. The end result is a reduced effective moment of inertia since all concrete below the neutral axis becomes ineffective due to cracking.

To develop moment curvature diagrams for a specific cross section, a minimum of four points are required to reflect changes in the material behavior: cracking of the concrete, yielding (or pseudo-yielding) of the reinforcing, strain hardening (or pseudo-strain hardening) of the reinforcing, and the point at which concrete crushes. The

contribution of concrete before cracking was also considered in this study. These four points make up the general moment curvature diagram.

Once these points are determined, a load deflection curve can be constructed for any location on the beam. The double integration method was applied to determine the load deflection curves at midspan for all beams. In this method the curvatures are applied as distributed loads on the test beam. The deflection at midspan of the actual beam can then be computed by integrating the curvatures twice over the test beam.

E. TEST SETUP AND DATA ACQUISITION

All beams were tested using a MTS Series 880 Universal Testing Machine. The MTS machine was modified with compression platens and a seven foot long W section steel beam to accommodate flexural testing of the reinforced concrete beams, as shown in Figure 13. Each beam was simply supported using pin and roller supports clamped to the W section. For the purpose of safety and lateral restraint, two wooden frames were attached with bolts to the W section. If any lateral movement was encountered during a test, the wooden frames would prevent any lateral movement until the test was terminated.

As mentioned earlier, standard hooks were used in the steel reinforced concrete beams to develop stresses. The hybrid FRP and unidirectional FRP rebars were sand coated in addition to being filament wound at the ends to provide some bearing capacity. To prevent longitudinal splitting of the concrete at the ends of the FRP reinforced beams (and subsequent pullout of the reinforcing), steel plates were clamped around the outside

of the beams at the support locations to provide confinement of the concrete. This approach proved, since none of the FRP reinforced beams exhibited pullout of the reinforcing.

Monotonic and repeated loading tests were performed on various test beams. To allow comparisons between repeated loading tests and monotonic tests, the envelopes of the repeated loading tests were determined by eliminating all load/unload data points. Load was applied at quarter points along the test beam using pin and roller supports, as shown in Figure 15. All monotonic tests were performed under displacement control at a rate of 0.0394 in/min. Repeated loading tests were also performed under displacement control at a loading rate of 0.0394 in/min, but an unloading rate of 0.197 in/min was used in the interest of time. Slow displacement rates were selected to ensure enough data collection during the test. Furthermore, unloading during a repeated loading test occurred when the midspan deflection of the test beam reached multiples of 0.12 inches. A stipulation of this type allowed for comparisons between the steel reinforced test beam and the hybrid FRP reinforced test beam.

The data collection was made using six linear variable differential transformers (LVDT), an MTS internal load cell, two dial gages, and a data acquisition system (Labtech). LVDT placement on the test beams are summarized in Table V.

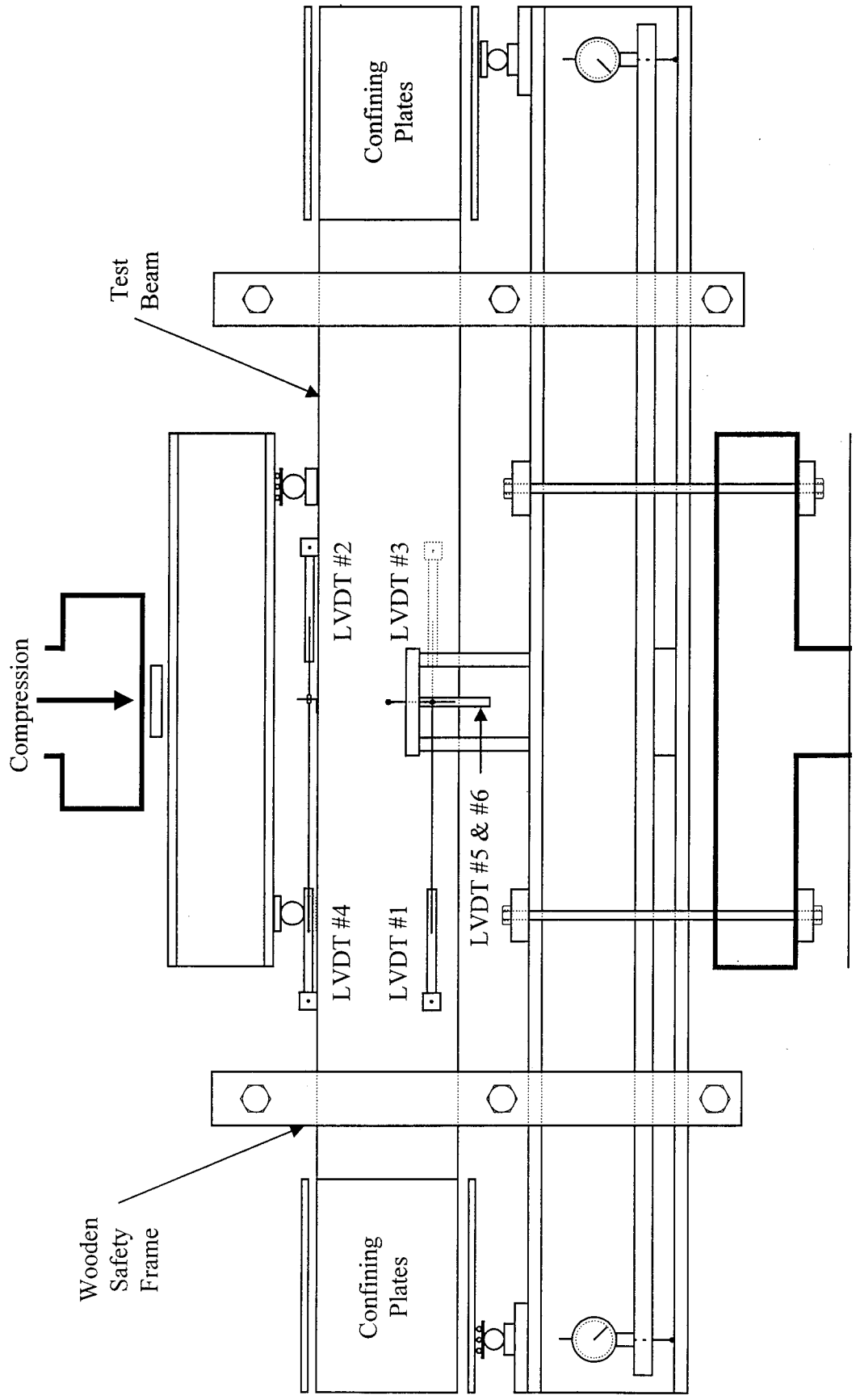

Figure 15 Beam Test Setup

In order to determine ductility in a reinforced concrete beam, the instrumentation of the test beams becomes very important. It is worthwhile to experimentally determine the curvature (or rotation) of the test beams so that the ductility of the beam can be determined. In research performed by Tholen and Darwin [19], linear variable differential transformers (LVDTs) were placed on the web to measure the deflections in the tension and compression regions of a given test beam. The measured deflections were then used to compute the rotation of the beam at the given location. In this project, a similar LVDT placement was used in the instrumentation of the test beams. However, a slightly different approach was taken to determine the experimental curvature values at a given moment.

Table V LVDT Placement

LVDT	Gage Length, in	Parameter Measured
LVDT #1	18	Tensile Strain
LVDT #2	9	Compressive Strain
LVDT #3	9	Tensile Strain
LVDT #4	18	Compressive Strain
LVDT #5	N/A	Midspan Deflection
LVDT #6	N/A	Midspan Deflection

To experimentally determine the curvature of the test beams, two strain measurements and the distance between them were required to construct a strain diagram at a given cross section. LVDTs #1 through #4 were placed in pairs to measure the tension and compression strain. A 9 inch gage length was selected to measure the strain

within the constant moment region, while an 18 inch gage length was chosen to ensure an average strain value reading. From the strain diagram, the location of the neutral axis was determined and the concrete compressive strain was computed using similar triangles. The curvature was then computed using Equation 8. To determine the corresponding moment at the measured strains, appropriate α and β_1 values were selected and Equation 7 was finally used to compute the moment capacity. Experimental and theoretical moment curvature diagrams are presented in the following section.

Midspan deflection was measured using LVDT #5 and #6. Since a direct measurement of deflection was performed, no calculations were required to compare the experimental results with the theoretical results. However, the stiffness of the beam test setup did affect the LVDT measurements. To account for the stiffness of the beam test setup, dial gages were placed to measure the deflection of the W section at the location of the test beam supports. Dial gage readings were recorded at different load stages, and a linear relationship between load and deflection was established. All theoretical load deflection curves were adjusted to account for this relationship so that a direct comparison between the theoretical and experimental load deflection curves could be made. These comparisons are presented in the following section.

All LVDTs and the MTS internal load cell were calibrated for use with the Labtech data acquisition program. During testing, Labtech was programmed to continuously collect data at a rate of one data point per two seconds for all LVDTs and the load cell.

F. RESULTS OF FLEXURAL TESTS AND DISCUSSIONS

The objective of the flexural testing program was to compare the behavior of various types and percentages of reinforced concrete beams. Theoretical and experimental moment curvature diagrams for each test beam along with the load deflection curves for each test beam will be used to evaluate the behavior of each beam. These comparisons will be beneficial in determining the future of the proposed hybrid FRP rebars.

1. Theoretical vs. Experimental Moment Curvature Diagrams. As discussed in previous sections, curvatures for each test beam were computed from the LVDT strain measurements. From similar triangles, strain measurements at the extreme concrete compression face and at the location of reinforcing were computed along with the location of the neutral axis. In addition, the experimental moments were computed from the experimental strain diagram. Therefore, all components of the experimental moment curvature diagrams were computed from strain compatibility.

The moment curvature diagrams of beam 1FRP1.0 are shown in Figure 16. Both the pseudo-yielding curvature and the ultimate curvature correlate well with the theoretical values. Furthermore, since moments were computed from the curvatures, the instrumentation of this beam accurately measured the experimental behavior.

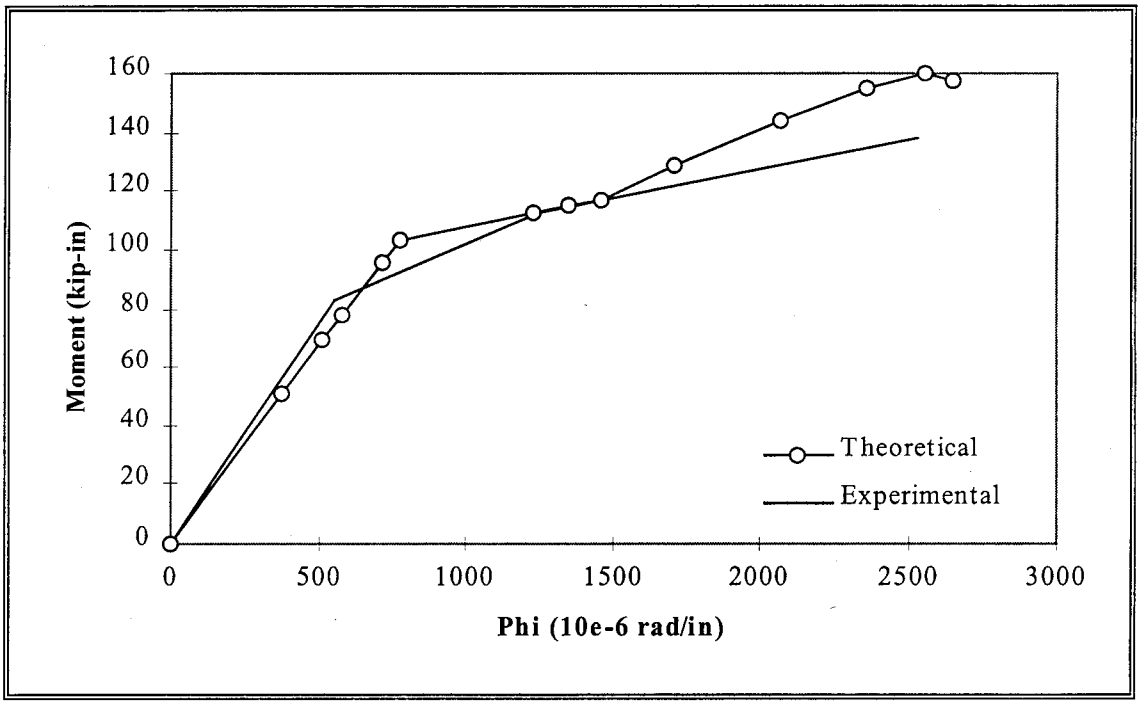

Figure 16 Beam 1FRP1.0 Moment Curvature Diagrams

The experimental moment curvature diagram for beam 3FRP1.5 did not correlate well with the theoretical. From the raw data, it was observed that the compression LVDTs did not accurately measure the compression strain. After testing, it was determined that both compression LVDTs were not instrumented properly; the connections between the LVDT and the mounting stud were such that small changes in the strain were inaccurately measured, as shown in Figure 17. A gap existed between the LVDT and the mounting stud which resulted in no strain readings until the gap was closed. By measuring less compressive strain, the neutral axis location was determined to be closer to the top of the beam than the theoretical neutral axis. The end result was an overestimation of the curvature and an underestimation of the moment capacity at a given curvature.

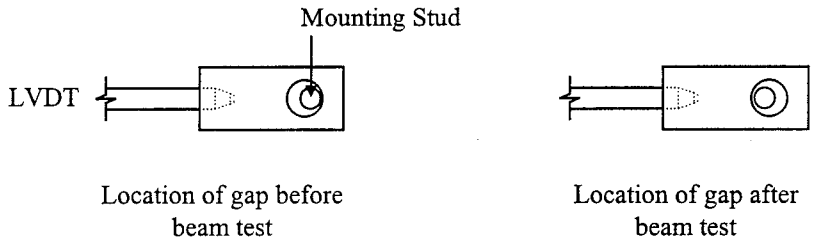

Figure 17 Gap Detail

For the remaining beam tests, the gap was eliminated by drilling a smaller hole in the LVDT bracket. This proved to be successful, as seen in the moment curvature diagrams of beams 2S1.7R and 4FRP0.5 (Figures 18 and 19). In both beam tests, the experimental moment curvatures correlated well with the theoretical moment curvatures. To visualize the benefits of the proposed hybrid FRP rebars, the experimental moment curvature diagrams were compared. Beam 1S1.0 was compared with beam 1FRP1.0, as seen in Figure 20. It is evident from the figure that beam 1FRP1.0 exhibited a pseudo-ductile range after pseudo-yielding. Since a small percentage of reinforcing was used in these beams, large ductility was expected; however, the rupture of the proposed hybrid FRP rebars controlled the failure of beam 1FRP1.0. If the rupture strain of the proposed hybrid FRP rebars was greater or the compressive strength of the concrete was less, additional ductility would have been measured, and a ductile failure would have occurred.

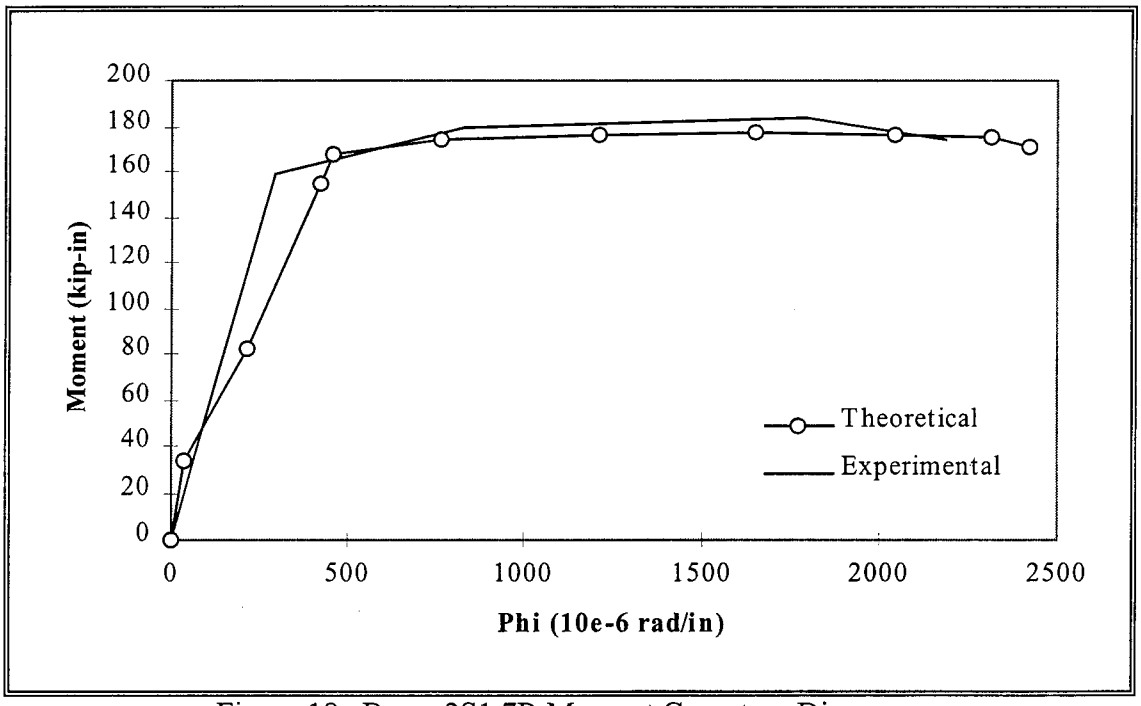

Figure 18 Beam 2S1.7R Moment Curvature Diagrams

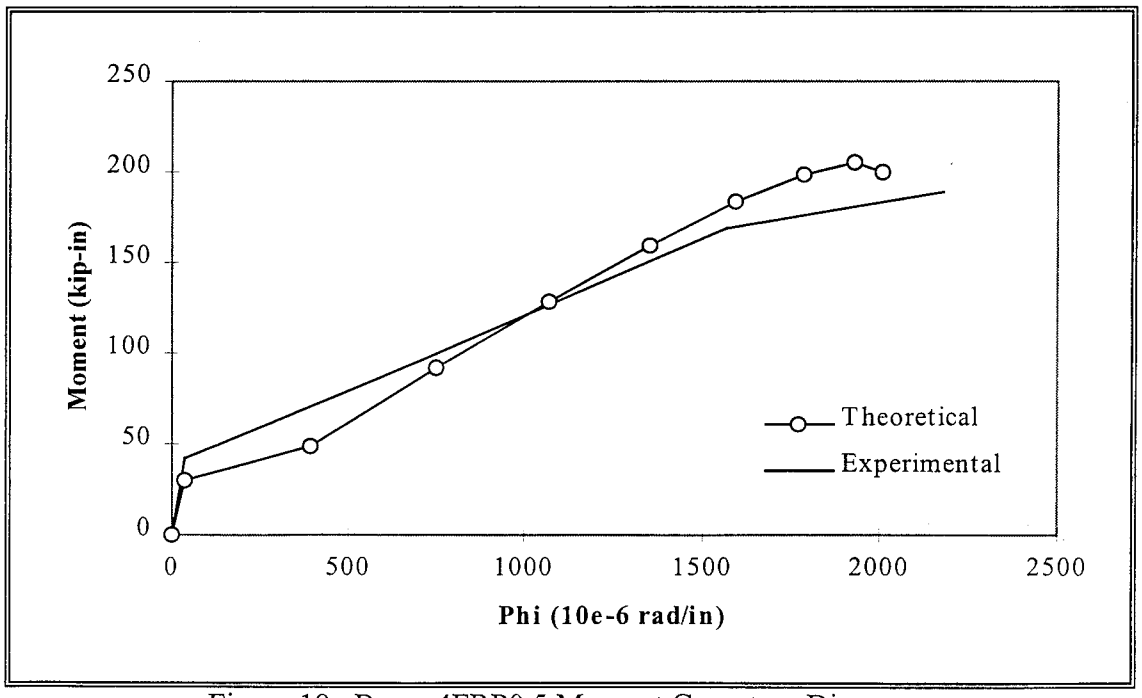

Figure 19 Beam 4FRP0.5 Moment Curvature Diagrams

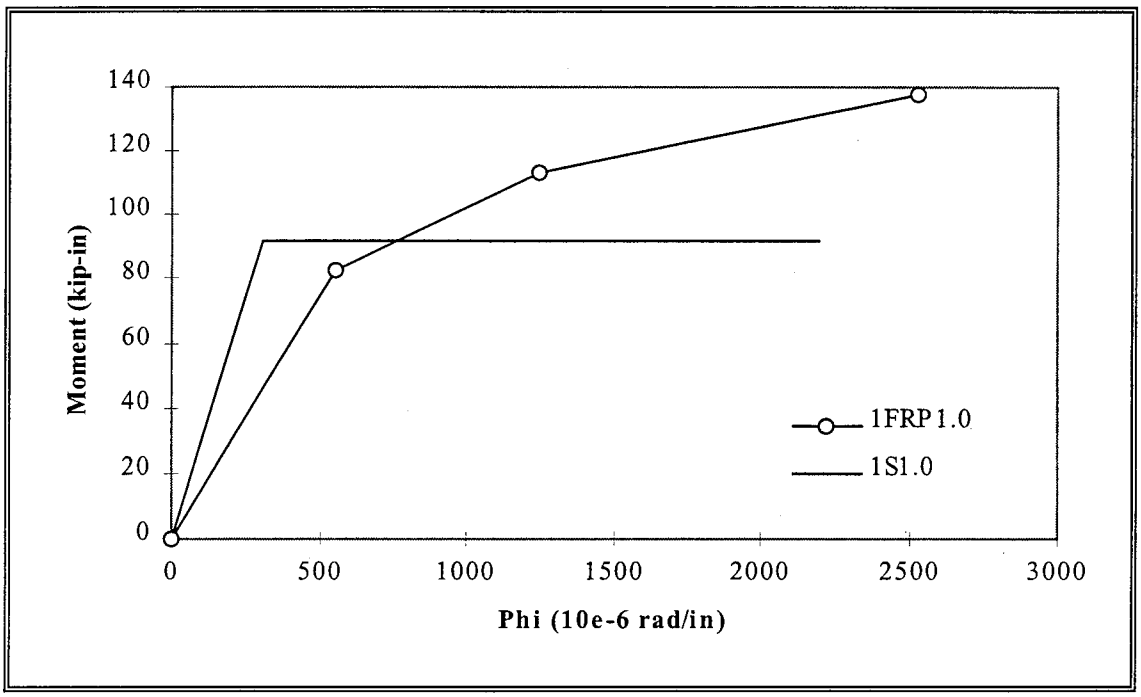

Figure 20 Steel vs. Hybrid FRP Experimental Moment Curvature Diagram Comparisons

Comparisons between unidirectional FRP and steel reinforced beams are presented in Figure 21. From these moment curvature diagrams, the lack of ductility using unidirectional FRP rebars is evident.

2. Theoretical vs. Experimental Load Deflection Curves. The following figures represent the load deflection curves for all monotonically tested beams. The load deflection curves for beam 1S1.0 are shown in Figure 22. As seen from the figure, the theoretical curve underestimated the actual behavior of the steel reinforced concrete beam; this is expected since the material behavior of concrete is taken to follow a parabola. The parabolic stress strain relationship underestimates the actual crushing strain of the concrete at the ultimate failure; therefore, the actual ultimate deflection was greater than expected. Furthermore, the effects of concrete stiffening are evident as seen

in the overestimation of the theoretical yield point. Beam 1S1.0 failed in a ductile manner, meaning the concrete crushed after yielding of the longitudinal steel reinforcing.

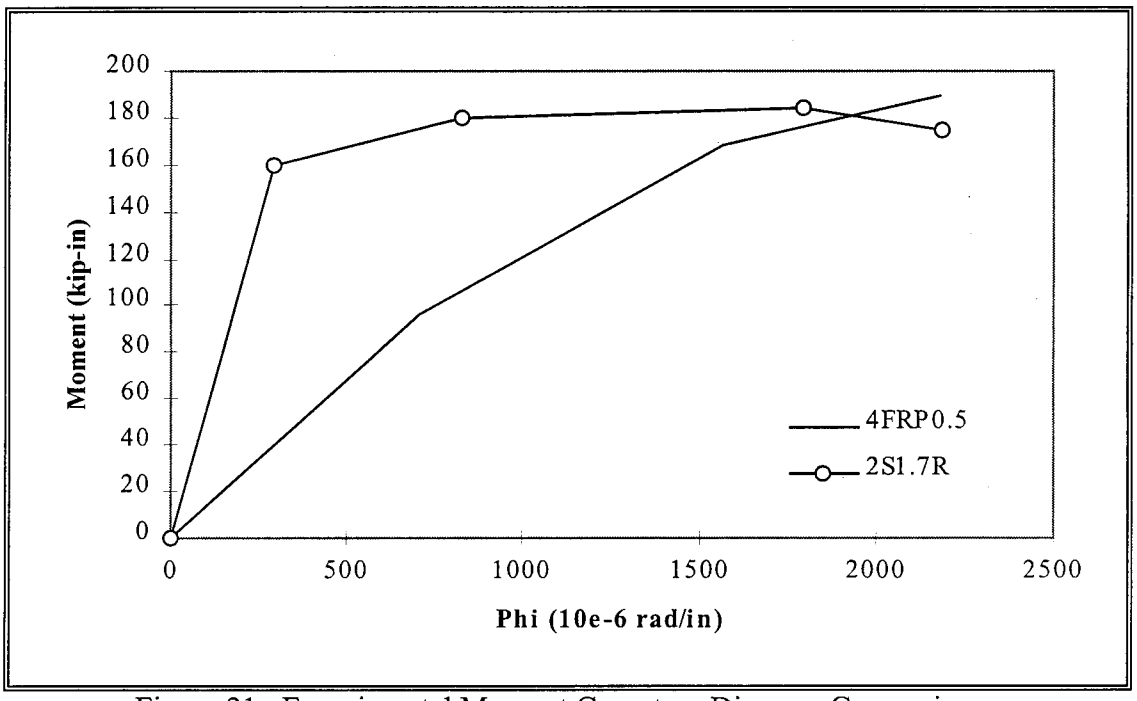

Figure 21 Experimental Moment Curvature Diagram Comparisons

The load deflection curves for beam 1FRP1.0 are presented in Figure 23. It is evident from Figure 23 that the theoretical model slightly overestimated the deflection at the pseudo-yield point; however this is advantageous since a larger pseudo-yielding plateau was experimentally obtained. Many more peaks occurred within the pseudo-yielding plateau; it is believed that this may be attributed to the concrete stiffening effect in much the same way that the concrete stiffening effect was used to explain the behavior of the proposed hybrid FRP rebars. Furthermore, additional cracking of the filament wound shell was also possible due to the increased length of the embedded hybrid FRP rebars.

During beam testing, each peak within the pseudo-yield plateau was accompanied by a loud noise, which was caused by cracking of the filament wound shell. Beam 1FRP1.0 exhibited a brittle failure mode; or rupture of the hybrid FRP reinforcing before crushing of the concrete, as seen in Figure 24. This failure mode could have been avoided if beam testing was performed at a lower concrete compressive strength of 4000 psi.

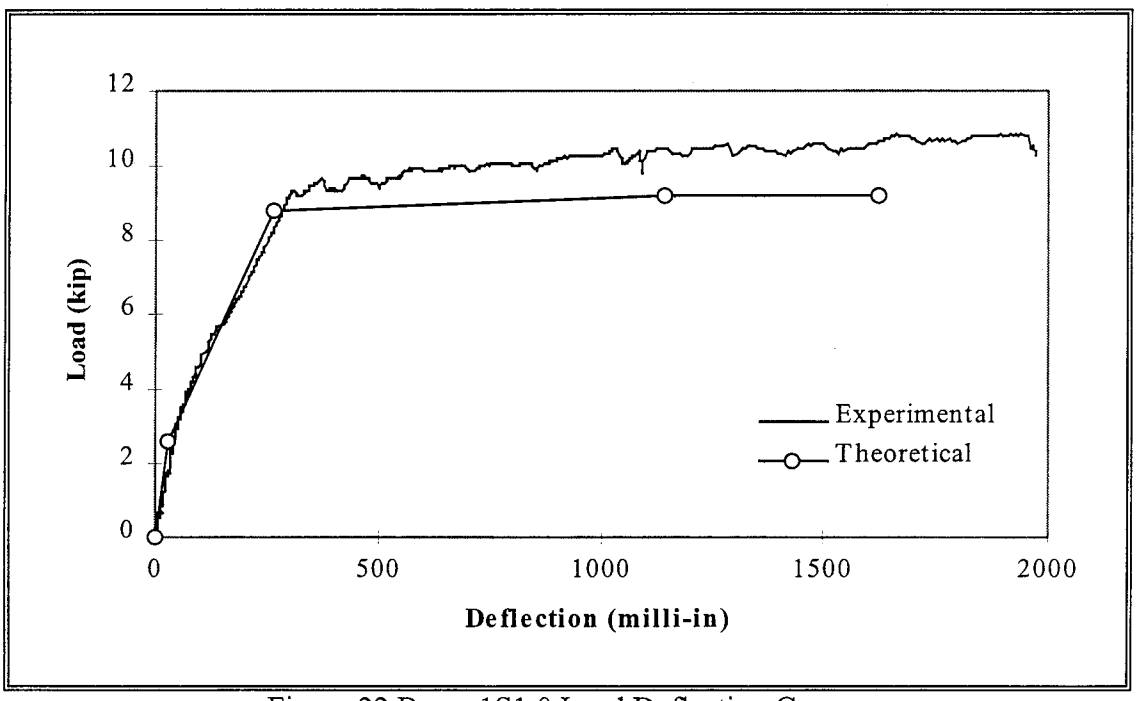

Figure 22 Beam 1S1.0 Load Deflection Curves

In contrast to beam 1FRP1.0, beam 3FRP1.5 failed in a ductile manner; as shown by the gradually descending portion of the load deflection curve, Figure 25. The theoretical load deflection curve corresponded very well with the experimental curve, with a slight deviation in the slope from cracking to pseudo-yielding. However, the ultimate load and deflection were both underestimated from the theoretical model. It is believed that this

underestimation of the ultimate load and deflection was due to the limitation of the ultimate concrete compressive strain of 0.0035 in/in.

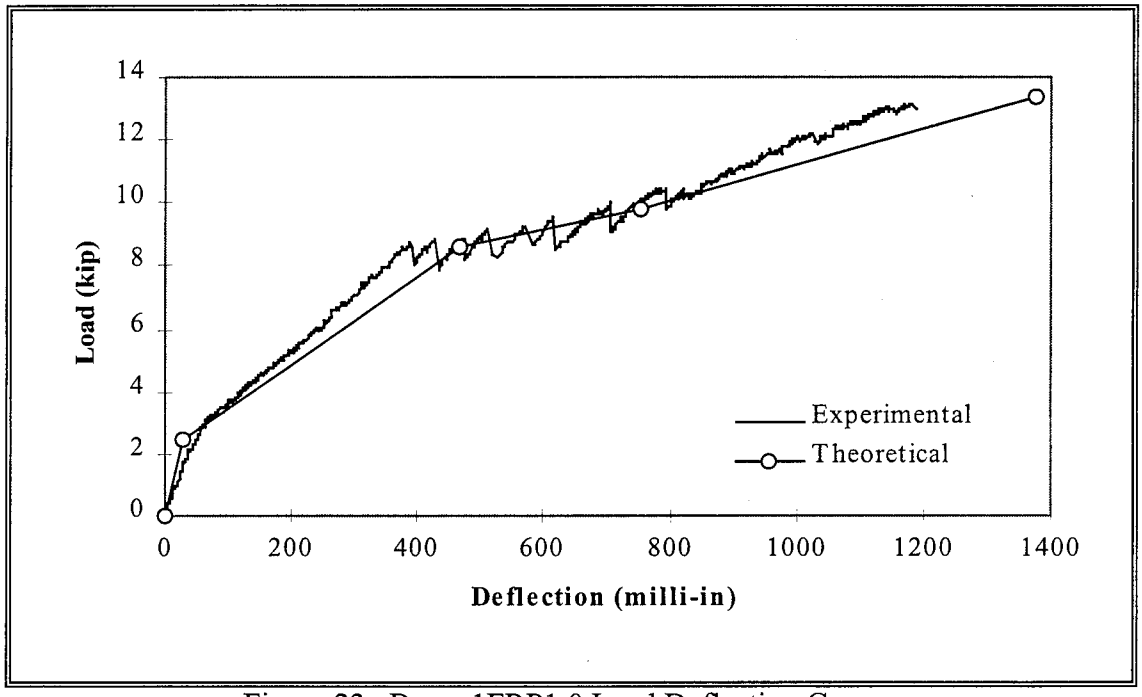

Figure 23 Beam 1FRP1.0 Load Deflection Curves

Beam 4FRP0.5 was a unidirectional FRP reinforced concrete beam; the reinforcing used followed a linear elastic stress strain relationship until rupture of the FRP. This linear elastic relationship is reflected in the load deflection curves, as seen in Figure 27. The theoretical load -deflection curve correlates well with the experimental results, considering the rule of mixtures was used to determine the behavior of the unidirectional FRP rebars. While the largest capacity was achieved using unidirectional FRP, no ductility was observed due to the linear elastic material properties. Furthermore, brittle failure occurred, with the test beam cracking into two separate fragments.

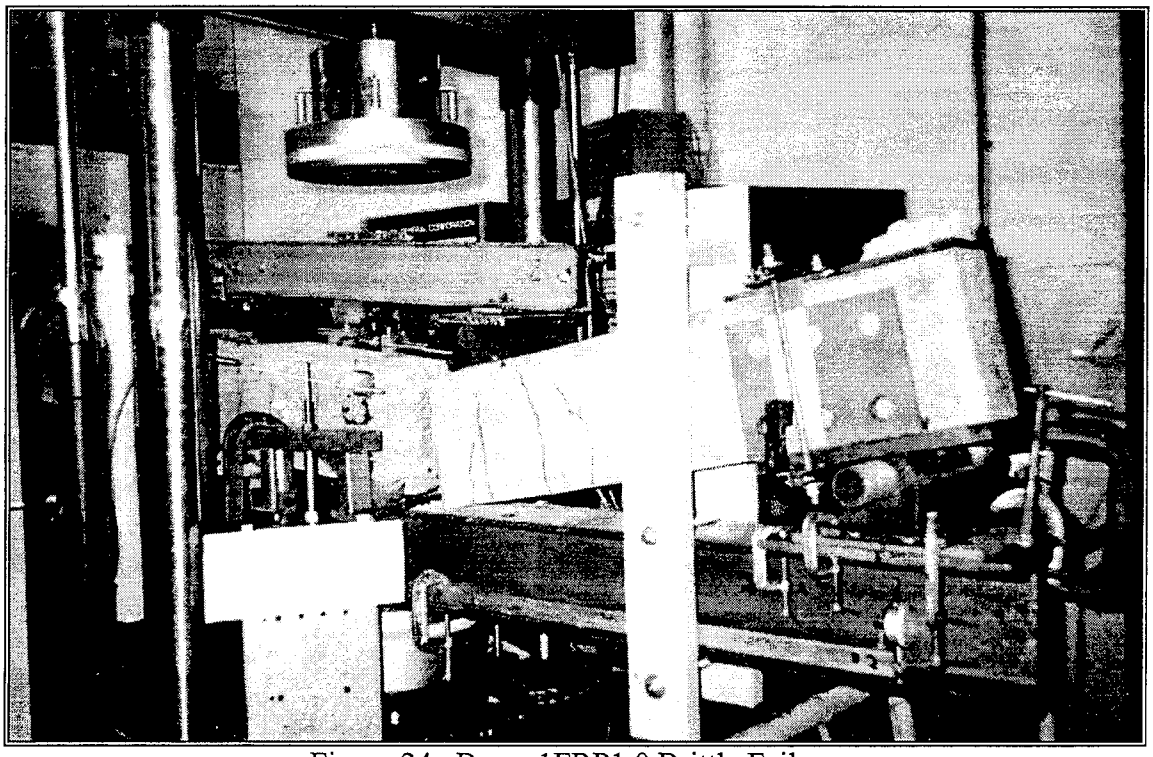

Figure 24 Beam 1FRP1.0 Brittle Failure

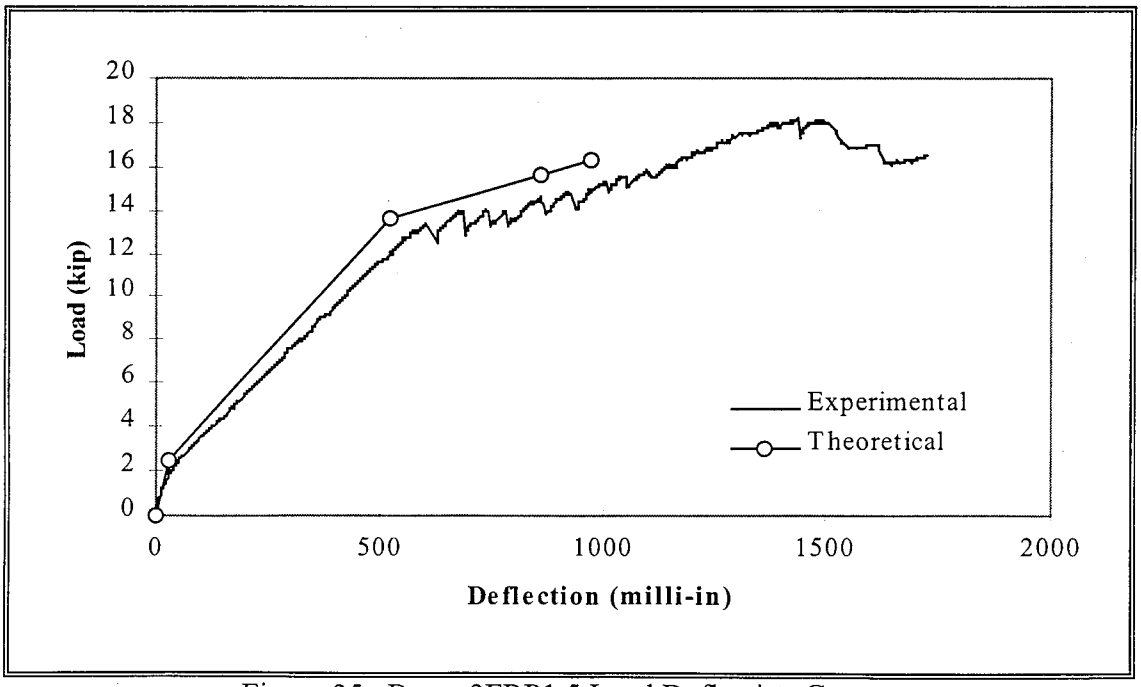

Figure 25 Beam 3FRP1.5 Load Deflection Curves

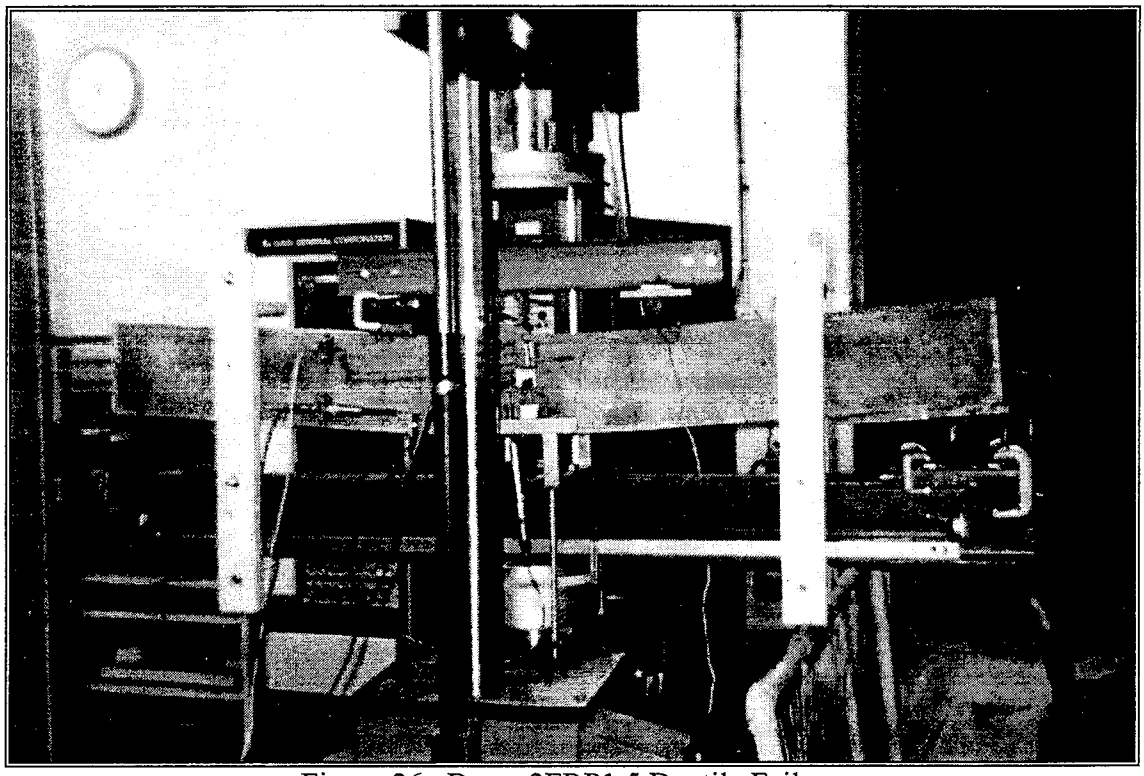

Figure 26 Beam 3FRP1.5 Ductile Failure

It is obvious that an allowable stress design approach should be imposed on unidirectional FRP rebars to account for the lack of ductility in the cross section. By providing an allowable stress limit, additional capacity is exchanged for the lack of ductility. Nonetheless, a brittle failure mode will occur with unidirectional FRP rebars, regardless of the allowable stress limit imposed.

As important as it is to theoretically determine the behavior of a reinforced concrete beam, it is also vital to present comparisons between different types of reinforcing. Figure 28 represents the experimental load deflection curves for beams 1S1.0 and 1FRP1.0. Ductility is evident in the hybrid FRP reinforced beam when

compared to the steel reinforced beam. In addition, the pseudo-strain hardening region of the hybrid FRP caused a large increase in the capacity of the beam near failure. Both beams were designed with approximately the same percentage reinforcing, yet there was a large difference in behavior due to the reinforcing material properties. As mentioned earlier, beam 1FRP1.0 did exhibit brittle failure, while beam 1S1.0 failed in a ductile manner.

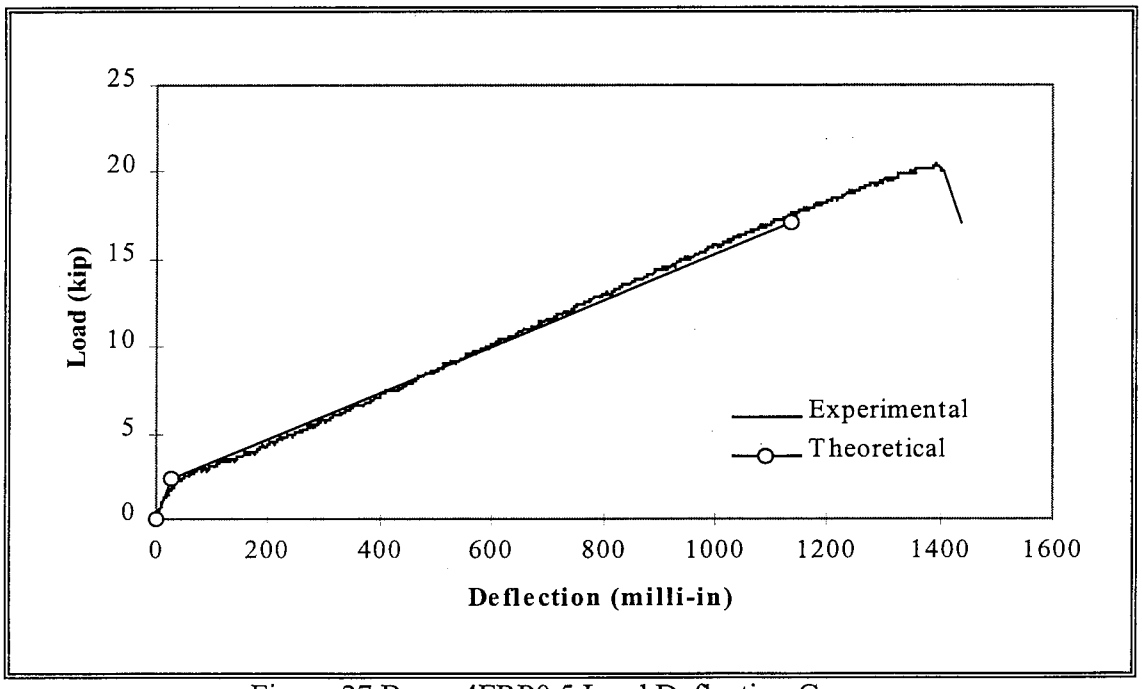

Figure 27 Beam 4FRP0.5 Load Deflection Curves

In contrast, the load deflection curves of beam 3FRP1.5 and 4FRP0.5 are shown in Figure 29. The pseudo-ductility gained by the proposed hybrid FRP is evident when compared to the behavior of the unidirectional FRP reinforced beam. Furthermore, ductile failure was observed in beam 3FRP1.5 as opposed to the brittle failure of beam 4FRP0.5.

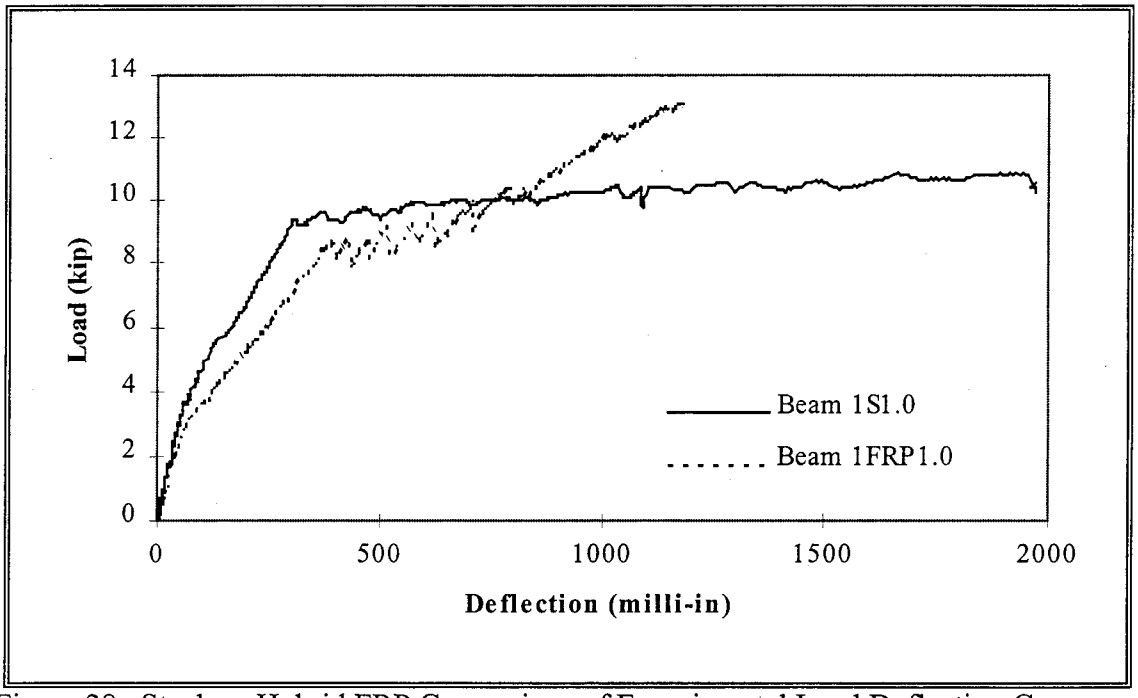

Figure 28 Steel vs. Hybrid FRP Comparison of Experimental Load Deflection Curves

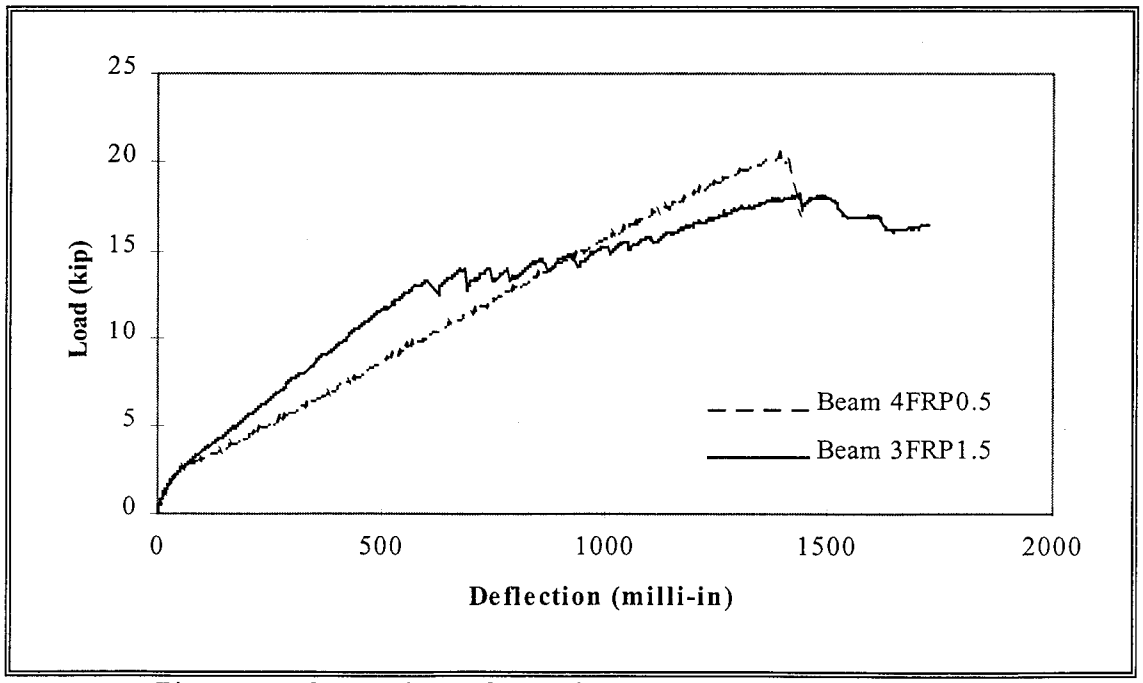

Figure 29 Comparison of Experimental Load Deflection Curves

Repeated Loading Test Results and Discussion. The load-deflection curves for beams 2S1.7R and 2FRP1.0R are shown in Figures 30 and 31, respectively. Each beam was loaded and unloaded ten times, then loaded to failure. However, every other repeated loading sequence was removed in the figures to make the curves more distinct. Beam 2S1.7R was a steel reinforced beam; under repeated loading large permanent deformations were evident after each repetition as seen in Figure 30. In addition, the slope of loading and unloading were the same, signifying no reduction in the stiffness of the reinforcing. On the other hand, beam 2FRP1.0R experienced decreased stiffness with each repeated loading sequence. The decreased stiffness was related to cracking of the filament wound shell. Furthermore, since the proposed hybrid FRP rebars consist of a linear elastic core, permanent deformation was less than the steel reinforced beam. Even after nine repeated loading sequences (Figure 32), the permanent deformation of beam 2FRP1.0R was only around 0.25 inches.

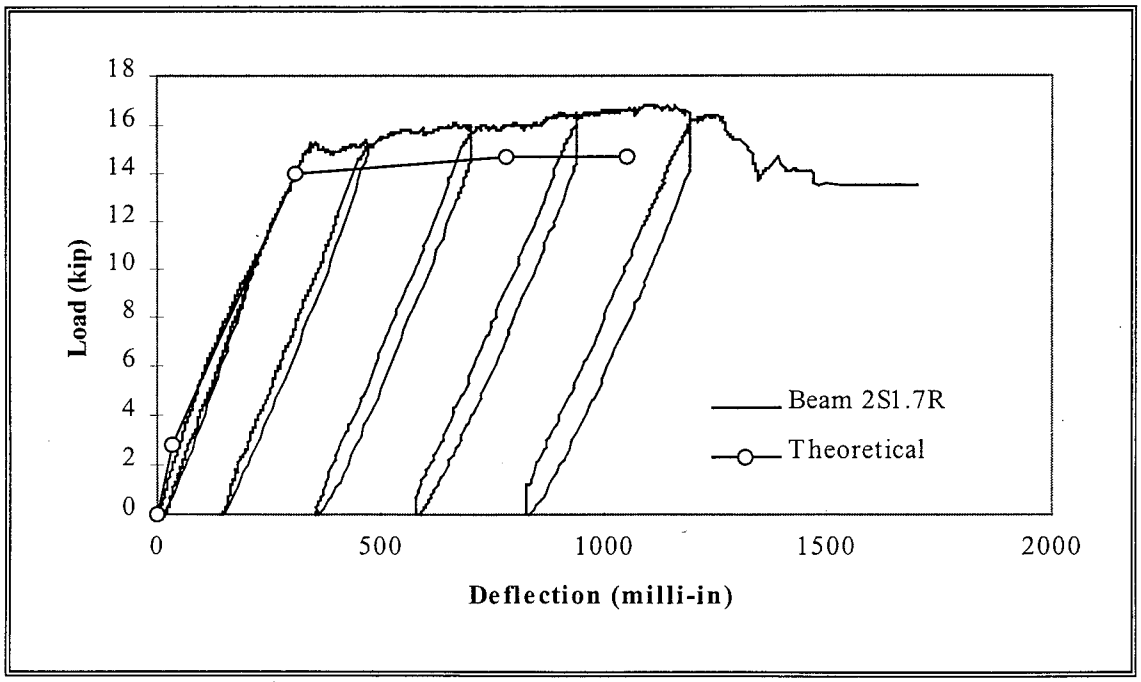

Figure 30 Beam 2S1.7R Load Deflection Curves

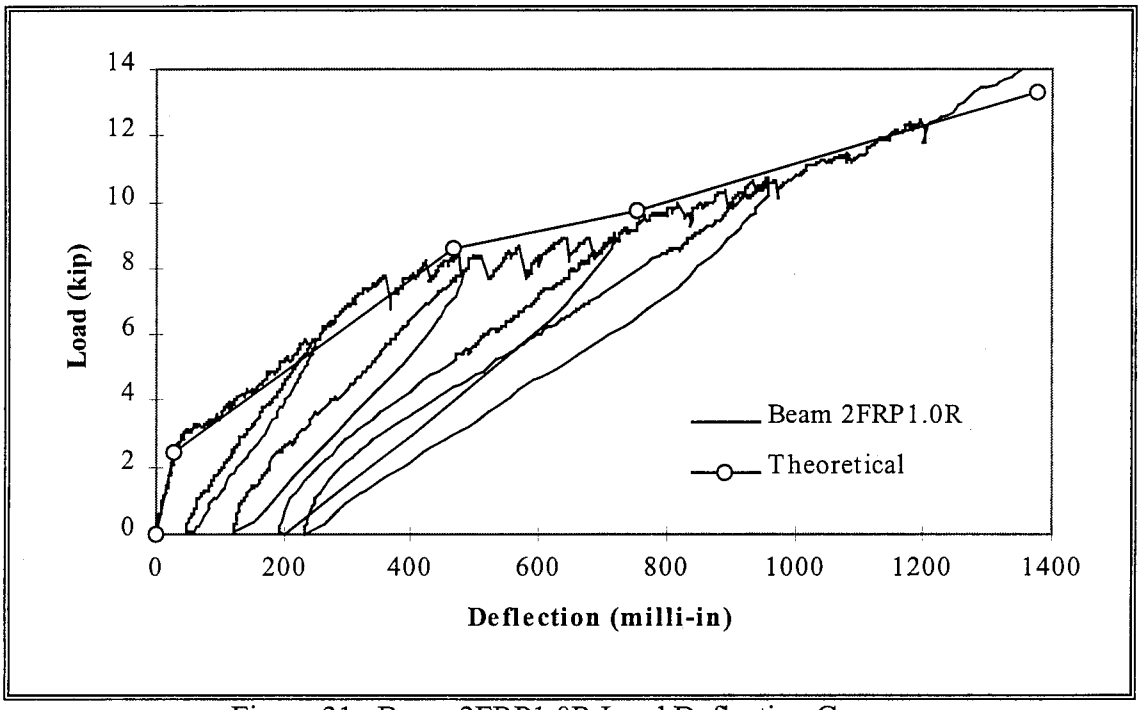

Figure 31 Beam 2FRP1.0R Load Deflection Curves

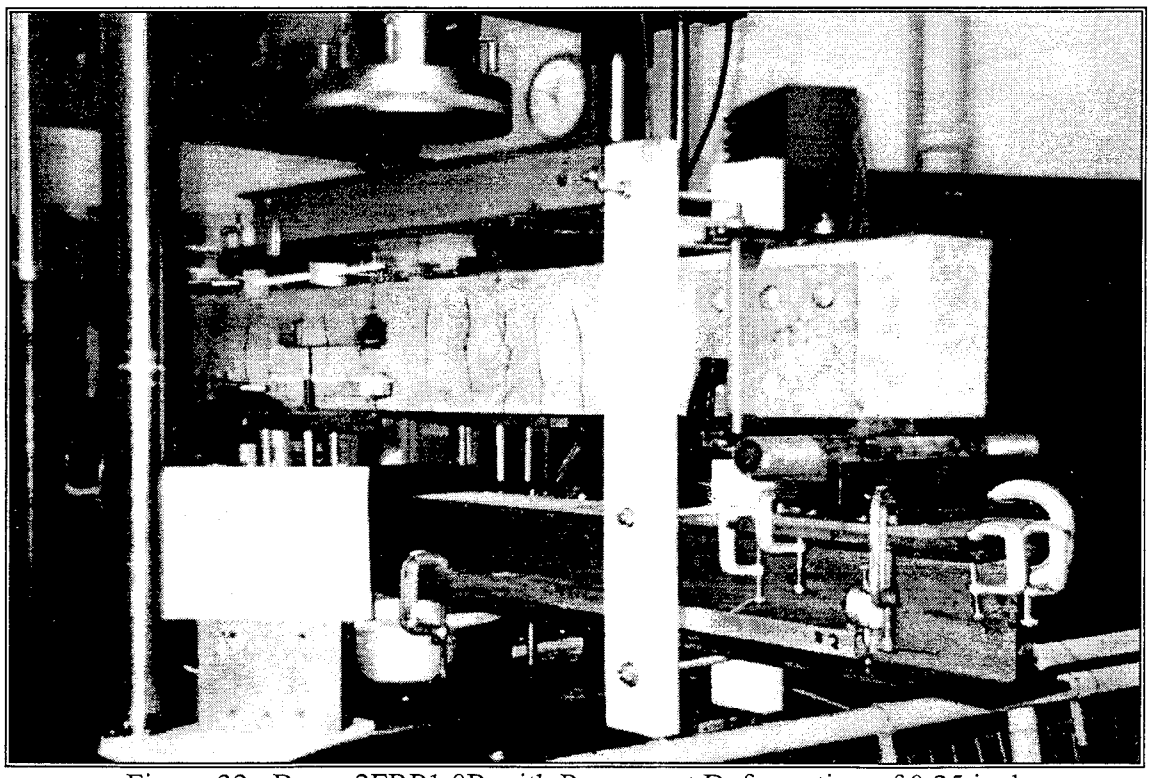

Figure 32 Beam 2FRP1.0R with Permanent Deformation of 0.25 inch

G. DUCTILITY INDEX

Since ductility is measured beyond the yield point of reinforcing in a concrete structure, energy methods can be useful to help describe the behavior of the structure. Any energy method usually requires an approximation or numerical integration of the area underneath a curve. The computed area is considered the energy absorbed by the system. For a ductile structure this area will be large, but for a brittle structure this area will be considerably less. In this study, the load deflection curves were used to determine the energy of the test beams. Naaman and Jeong [20] define a ductility index based on the energy computed from load deflection curves:

$$\mu_w = \frac{1}{2}\left(\frac{W_{tot}}{W_{el}} + 1\right) \qquad (9)$$

where W_{tot} is the energy computed up to failure, and W_{el} is the energy computed for the elastic portion of the load deflection curve. This allows direct comparisons of ductility between test beams regardless of their material and geometric properties.

In addition to ductility based on energy, another measure of ductility can be computed from the load deflection curves. The ductility based on deflections follows Equation 10:

$$\mu_\Delta = \frac{\Delta_u}{\Delta_y} \qquad (10)$$

where Δ_u is the ultimate deflection and Δy is the yielding deflection.

A summary of the ductility indexes for the test beams is shown in Table VI. From the table, the lack of ductility in unidirectional FRP reinforced beams is evident, since no post yielding behavior is observed. This results in a ductility index of 1.0 for any unidirectional FRP, unless an allowable stress limit is placed on the reinforcing. In contrast, the steel reinforced beams exhibit high ductility indexes, due to the small energy required to achieve yielding in the rebars and the large yielding plateau of steel. Finally, the ductility indexes of the hybrid FRP reinforced beams demonstrate their effectiveness in providing pseudo-ductility to a concrete structure. With modifications to the engineering properties of the proposed hybrid FRP rebars in the future, ductility comparable to that of steel will be possible.

TABLE VI Summary of Ductility Indexes

Beam	Ductility μ_w	Ductility μ_Δ
1S1.0	6.10	6.72
2S1.7R	4.43	5.10
3S2.0	2.81	2.75
1FRP1.0	3.31	3.05
2FRP1.0R	3.93	3.85
3FRP1.5	3.02	3.10
4FRP0.5	1.00	1.00
5FRP1.8	2.40	2.20
5FRP1.8	2.62	2.33

H. FIBER OPTIC SENSORS

Strain sensing in FRP structures and concrete structures has been done with in-situ fiber optic sensors. These sensors have found increasing applications in development of smart structures because of advantages including compatibility with host

structures and the ability to be multiplexed [21,22]. The technology allows the measurement of internal strains and has the potential for long-term monitoring. A smart FRP rebar can give quantitative assessment of internal loading and damage. In this study, fiber optic sensors were placed inside FRP rebars, which in turn were placed in concrete beams. The sensors monitored strain during load tests and indicated the cracking events and the subsequent redistribution of load in the rebar.

Extrinsic Fabry-Perot interferometric (EFPI) single-mode fiber optic sensors were used to measure strain in FRP rebars [7]. These sensors were incorporated in the mid-length of the rebars during fabrication and were located between the pultruded core and the helical windings. The optical fiber lead for the sensors exited one end of the rebars through a protective plastic tube. The tube extended about a centimeter inside the rebar. The sensors were 250 micrometers in diameter and had a negligible effect on the rebar structure [23].

EFPI sensors consist of two glass fiber wave-guides inserted in a low-profile glass capillary tube. The end faces of the inserted fibers form a small cavity and are polished and coated for high reflectivity. Optical interference between reflections from the end faces is dependent on the cavity size. Longitudinal strain of the capillary tube induces a nonlinear optical interference signal. The operation of the sensors is described in the literature [22]. These sensors are environmentally rugged, are immune to electrical interference, are highly sensitive, and are compatible with FRP structures.

The optical sensors and instrumentation, in this study, were manufactured by Fiber and Sensor (F&S) Technologies. FOSS models were used with an optical wavelength of 1310 nm. Three EFPI sensors were numbered # 1, #2, and #3 and had gauge lengths of 4.66 mm, 5.01 mm, and 4.89 mm. respectively. They were demodulated using a fringe counting technique with strain resolutions of 35 me, 33 me, and 33 me, respectively [7]. The instrumentation consisted of a laser diode optical source, a 3 dB fiber bi-directional coupler, and a high speed photodetector. The modulated optical

sensor data reliably indicated the occurrence of cracks and the subsequent redistribution of load in the rebar. The sensors reflected the different strain conditions in rebar at different locations in the concrete beam. Unfortunately, the sensors did fail at cracking of the FRP shell. The maximum strain that was recorded by fiber optic sensors corresponded to pseudo-yield of FRP rebars. The failure of the fiber optic occurred at the first crack of the FRP shell since this later was placed at the core shell interface. Future manufacturing of FRP rebars is considering the placement of the fiber optic within the FRP core. Overall, the study demonstrated the usefulness of fiber optic sensors for monitoring internal strain in reinforced concrete subject to large deformation.

I. BOND PERFORMANCE OF FRP REBARS

The objective of this study was to study the bond performance of FRP rebars that were manufactured at UMR. Rebars should have good bond characteristics to adhere to concrete under tensile loading. In general, the bar-concrete bond mechanism includes three different components: adhesion, friction, and interlock. Bar-concrete adhesion is a bond due chemical adhesion developed at the bar-concrete interface. Adhesion does not provide a significant contribution to bond and depends on the bar-surface texture. Bar-concrete friction is the bond component due to forces parallel to the bar axis. Usually smoother bar gives low frictional forces. For a bar with rough surface such as ribs in today's steel bars, when the bar tends to slip, the concrete between the ribs is subjected to shear and provides a bar-concrete interlock bond, which depends on the bar-rib geometry.

The FRP rebars made at UMR, as discussed previously, are manufactured through pultrusion for the core and filament winding for the shell. The shell, will have then, an

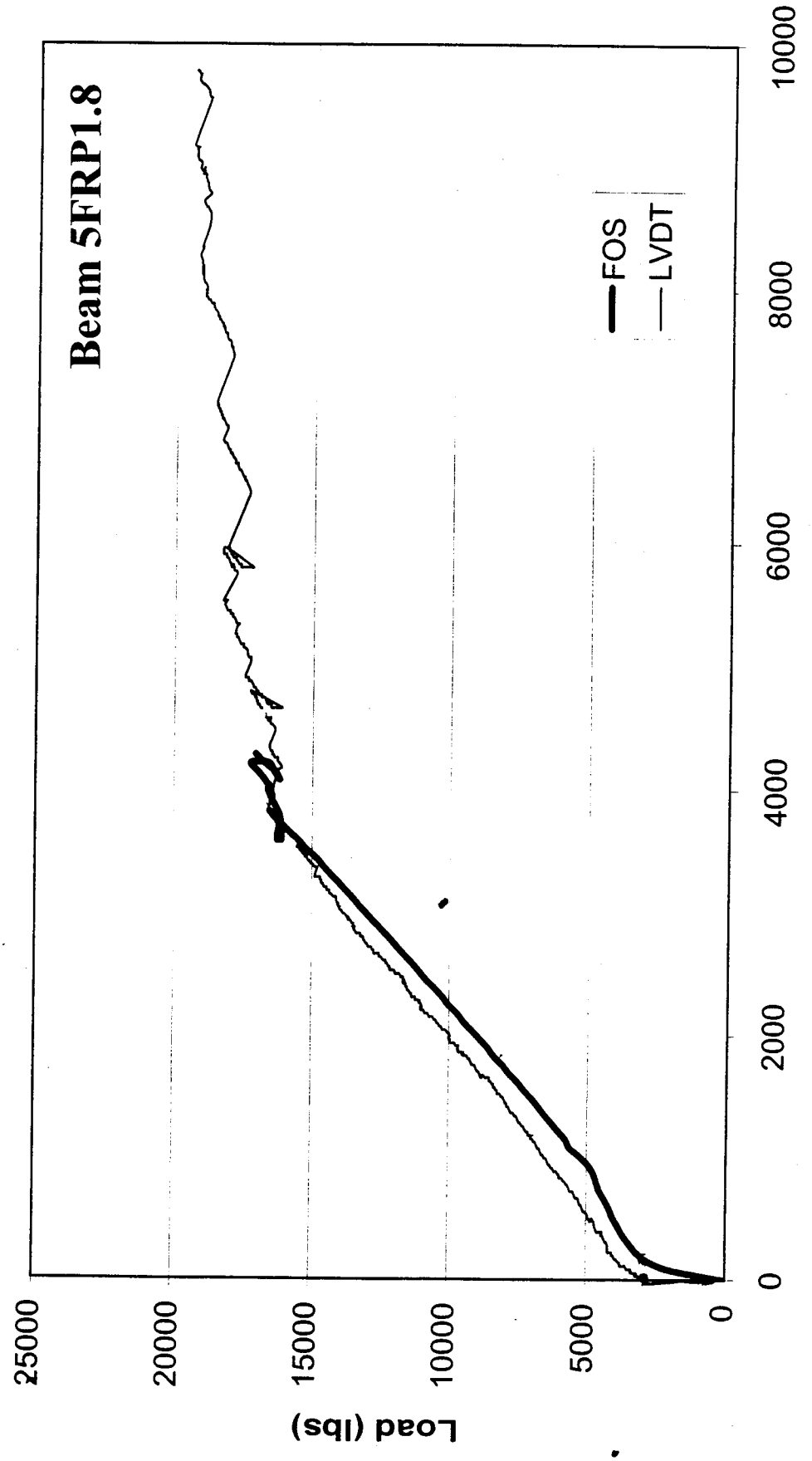

Figure 33 Comparison of strains Measured by LVDTs and Fiber Optic Sensors for Beam 5FRP1.8

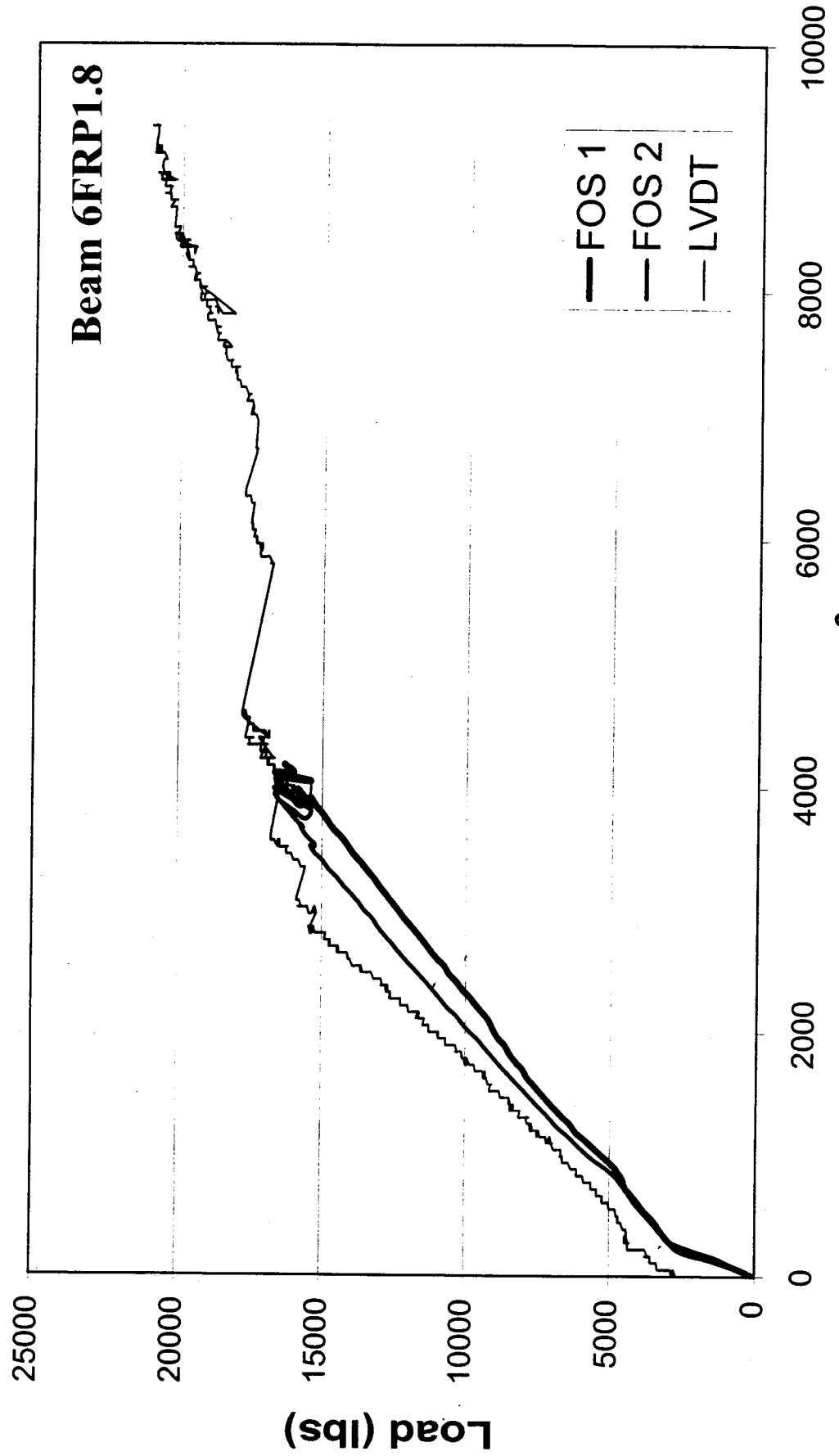

Figure 34 Comparison of strains Measured by LVDTs and Fiber Optic Sensors for Beam 6FRP1.8

irregularity in the surface providing semi-rib texture. In addition, the surface is sand-coated to enhance the frictional force component.

The study of bond of particular reinforcement type can be very comprehensive by including the investigation of so many parameters such as, rebar type, rebar, size, embedment length, concrete strength, loading rate, etc. The scope of this study was limited and the objective was to provide a qualitative information about the FRP rebar characteristics as compared to steel rebars. All the FRP rebars produced for this study have a size comparable to number 3 steel rebars and a pseudo-yield stress comparable to grade 40 steel. Therefore, the study focussed on quantitatively determine the bond stress of both FRP rebars and companion steel rebar and compare the results based on bond strength and failure modes and draw conclusions and make recommendations.

1. Test Specimens and Materials. Twenty-four coupons were tested for bond characteristics (see Table VII). All test were pullout of rebars embedded in with embedment lengths were chosen to be 3 i. And 6 in. Nominal bond strength, slip at the onset of failure, mode of failure, and nominal bond stress-slip relationships were obtained from pullout tests of FRP rebars, and they were compared to pullout tests for steel rebars. The specimens were prepared using 6x12 inch steel cylinders. Before rebar placement the molds were cleaned and oiled. The rebar was placed axisymmetrically in the molds. Steel rebars and FRP rebars were used with length of four feet to provide ample length for gripping during testing. A list of the specimens included in this study are shown in Table VII. Two concrete strengths namely 5500-psi and 9000-psi were included. Rebar embedment lengths were 3 in. and 6 in. FRP rebars were manufactured with shell that consist of one round of filament winding (specimens **1**-3xx and **1**-6xx), two rounds of filament winding (specimens **2**-3xx and **2**-6xx) and some rebars with the

surface being sand coated (specimens 1-3**s**, 1-6**s**, 2-6**s**). All steel rebar specimens were labeled **s**-xx.

During the making of test specimen the rebars were restrained at both ends to keep the bars from moving during the pouring of the cylinders. To accomplish this a ¾ in x 1 ½ in block of wood was placed in the bottom of the mold. This block had a hole in the center, sized to accept a length of PVC pipe. The pipe was placed on the end of the bars and sealed with silicone to adjust the embedment length as shown in Figures 35 and 36. A wood rack was built and placed over the molds to hold the rebar at the top as shown in Figure 37. This preparation was done 24 hours prior to the pouring of the specimens to provide time for the silicone seal to dry.

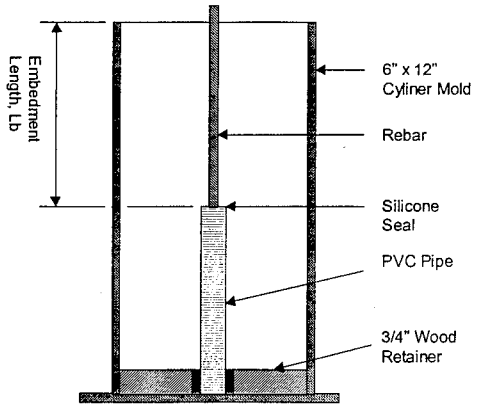

Figure 35 Side View of the Mold Setup

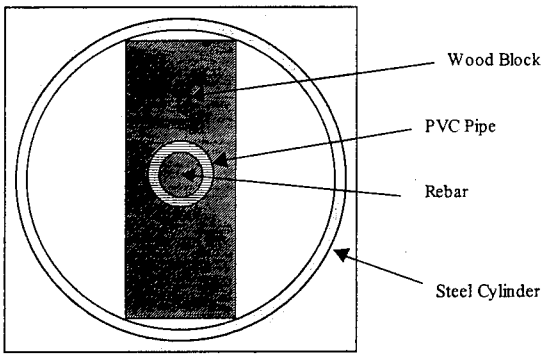

Figure 36 Top View of the Mold Setup

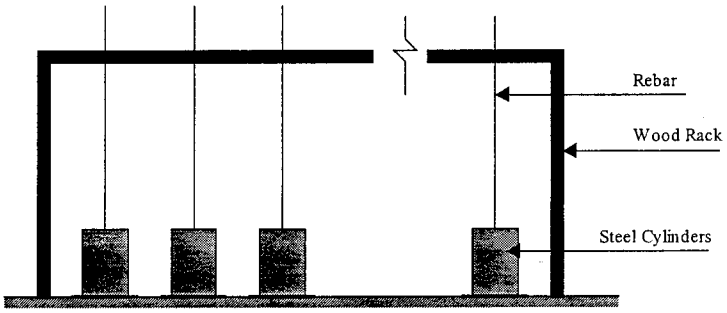

Figure 37 Drawing of the Rack Used to Hold the rebar Vertical During Pouring

2. Test Setup. The testing was performed at least 28 days after the pouring of the specimens. The test was set up as shown in Figure 38. The specimen was placed on top of a universal testing machine and resting on a ½ inch thick bearing plate. The plates used for all rebars had a 1 ½ inch hole in it. The rebar extended down and was gripped below. Two LVDTs of 0.001 inch range were placed at each end of the rebar to measure the slip occurring during the testing.

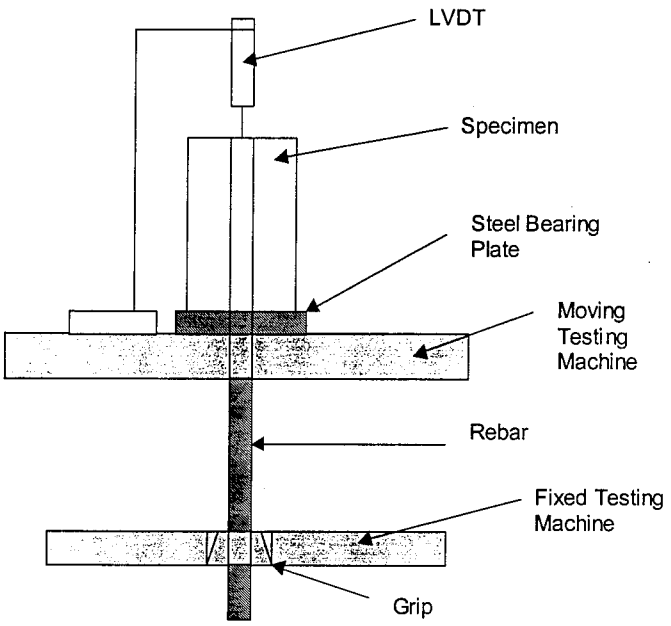

Figure 38 Schematic of Test Setup

During the loading of the cylinders, rebar displacement was measured continuously as mentioned above using LVDTs. LVDT 4 was placed at the bottom of the rebar inside the cylinder (where a hole had been chipped away in the plastic sleeve) and LVDT3 was placed at the top of the cylinder.

3.Test Results. In the pullout tests, measurements of load and displacement were taken at the rate of 1 data point per second during the monotonically increasing load process. The load and displacement values were used to calculate the appropriate nominal normal stress, nominal bond stress, and the slip for each bar. Normal stress were calculated as the recorded pullout

force divided by the nominal cross section of the rebar,. The values of the nominal bond stress were calculated by dividing the same recorded pullout force divided by the surface area of the bar embedded in the cylinder. For slippage, it was most logical to use the displacement measurements of LVDT 4, which actually recorded the movement of the bottom of the rebar inside the cylinder, as the total slip. In comparison to other methods that have been used to measure total slippage, this value was compared to the total displacement of LVDT 3, placed 8 inches from the top of the concrete, minus the actual elongation of the rebar recorded by the extensometer.

When comparing the bond stress of all specimens as shown in Table VII, results reveal that FRP rebars provide slightly less bond resistance as compared to steel bar. The maximum nominal bond stress is determined only when the rebar pulls out of concrete. If a rebar yield without pullout, the corresponding bond stress is not necessarily the bond resistance of that particular reb, such as the case of specimens s-6a and s-6b. Most of the FRP rebars did reach their pseudo-yield stress before pull out. This indicates that the bond stress recorded during tests are not the maximum bond stresses. Having used smaller embedment lengths would have resulted in higher bond stresses. The difference in mode of failures between steel rebars and FRP rebars is mainly observed in the post yield region. When the steel rebar yield, it continues to deform without pullout, however, the FRP rebar may end up with pullout just after the firs yield (or crack of the shell). All the pullouts noticed in FRP beams were due to the pullout of the core from the shell after some cracking of the shell. However the shell maintained its adherence to concrete. This phenomenon was not observed in the beam tests since the rebars did not have free ends. FRP shell, in beams, continued to crack at concrete crack locations. Out of all the tests carried in this study, two of the specimens failed at the grip, the others all pulled

out of the concrete. Overall, the FRP rebars exhibited adequate bond resistance, especially, the sand coated rebars. The lack of bond was more at the core-shell interface rather that concrete-rebar interface. However, all bond damage of the core-shell interface occurred after pseudo-yield of the FRP rebars.

TABLE VII Summary of Bond Test results

Specimen Name See above	Concrete compressive strength f'c (psi)	Embedment length (in)	MAX Load (lbs)	Maximum Normal stress (psi)	Maximum Nominal Bond Stress (psi)	Measured total deformation outside cylinder (LVDT3) (in.)	Measured Total slip inside cylinder (LVDT4) (in.)
s-3a	6136	3	5811	52640	**1645**	.385	.354
s-3b	6136	3	6043	54742	**1711**	.351	.136
s-3c	9000	3	5329	48274	**1506**	.057	0
s-6a	6136	6	6956	63013	**985**	.39	.02
s-6b	6136	6	6973	63167	**987**	.342	.017
s-6c	9000	6	5230	47377	**740**	.115	.002
1-3a	5271	3	4283	38799	**1212**	.218	.349
1-3b	5271	3	4765	43165	**1349**	.19	.186
1-3sa	5271	3	4997	45267	**1415**	.055	.176
1-3sb	6136	3	4482	40601	**1269**	.021	.03
1-3sc	9000	3	6375	57750	**1805**	.184	.237
1-6a	5271	6	5346	48428	**756**	.109	.208
1-6b	5271	6	6060	54896	**858**	.835	.44
1-6sa	5271	6	3320	30075	**467**	.067	.002
1-6sb	9000	6	6259	56699	**886**	.438	.242
1-6sc	9000	6	5545	50231	**785**	.231	.535
1-6sd	9000	6	7072	64063	**1001**	.019	.001
2-6a	5271	6	6823	61808	**966**	.94	.668
2-6b	6136	6	5014	45420	**710**	.385	.009
2-6sa	5271	6	7288	66020	**1032**	1.148	.621
2-6sb	6136	6	4416	40003	**625**	.189	.351
2-6sc	9000	6	6541	59253	**926**	.992	.489
2-6sd	9000	6	5960	53990	**844**	.917	.599
2-6se	9000	6	5761	52187	**815**	.52	.129

J. CONCLUDING REMARKS

The beam testing program was successful in proving the pseudo-ductility of the proposed hybrid FRP rebars embedded in concrete. Excellent agreements with theoretical curves were obtained for all experimental load deflection curves. However, faulty instrumentation of some of the test beams prevented the experimental moment curvature diagrams to exhibit similar agreements with theoretical diagrams.

Furthermore, the advantages of structural health monitoring by using fiber optic sensors embedded within the hybrid FRP rebars has been demonstrated through the preliminary fiber optic sensor testing program. The sand-coated rebars also showed adequate bond resistance.

VI. CONCLUSIONS

A. CONCLUSIONS

Both the tensile coupon testing program and the beam testing program concluded a comprehensive investigation of the manufacture and application of the proposed hybrid FRP rebars. The following conclusions were drawn from all investigations.

1. Combined Pultrusion and Filament Winding Process. The combined pultrusion and filament winding process ensured symmetric fiber placement over the cross section of the rebar. The application of filament winding was vital in obtaining symmetric fiber placement. Furthermore, symmetric fiber placement made the unique stress - strain behavior of the proposed hybrid FRP rebars possible.

2. Tensile Testing of the Proposed Hybrid FRP Rebars. All tensile coupon testing exhibited repeatable stress strain behaviors. A pseudo-ductile region was observed in all tensile coupon tests. An analogy to concrete stiffening provided a simple yet concise explanation of the stress strain behavior. By altering the fiber types and their corresponding volume fractions, a hybrid FRP rebar with the engineering properties of virtually any material may be achieved.

3. Flexural Testing of Hybrid FRP Reinforced Beams. Flexural testing of hybrid FRP reinforced beams confirmed the pseudo-ductile characteristics of the proposed hybrid FRP. Furthermore, comparisons between steel reinforced and unidirectional FRP reinforced beams were valuable in showing the differences in behavior of various types of reinforcing. Finally, repeated loading tests confirmed the permanent residual deformation of the hybrid FRP reinforced beams; a behavior typical of steel reinforced beams.

4. Ductility Index. Two different computations of ductility establish the pseudo-ductility evident in the proposed hybrid FRP rebars. It was also proven that currently available unidirectional FRP reinforcing does not provide ductility after post-yielding; thus a requirement of an allowable stress approach for current FRP is required.

5. Health Monitoring. The EFPI optical strain sensors survived the rebar and beam fabrication steps and operated during most of the load tests. The optical sensors did not fail until severe cracking of the concrete beam and the FRP rebar. The sensor data reliably indicated the occurrence of cracks and the subsequent redistribution of load in the rebar. The sensors reflected the different strain conditions in rebar at different locations in the concrete beam. The study demonstrated the usefulness of fiber optic sensors for monitoring internal strain in reinforced concrete subject to large. Furthermore, the advantages of structural health monitoring by using fiber optic sensors embedded within the hybrid FRP rebars has been demonstrated through the preliminary fiber optic sensor testing program.

6. Bond Resistance. The FRP rebars exhibited adequate bond resistance at the concrete-rebar interface. Bond stresses were comparable to those of companion steel coupons. Furthermore, all FRP rebars failed by yielding before pullout and the pullout occurred at the core-shell interface, which showed that bond failure may occur in the rebar itself that at the concrete surface.

REFERENCES

1. Xiao, Y., "Shear Retrofit of Reinforced Concrete Bridge Piers Using Prefabricated Composites," *Fiber Composites In Infrastructure*, ICCI'98, Tucson, Arizona, January 1998, pp. 221-233.

2. Argawal, B.D. and Broutman, L.J., *Analysis and Performance of Fiber Composites*, John Wiley & Sons Inc., New York, 1990, 449 pp.

3. Belarbi, A., Chandrashekhara, K., and Watkins, S., "FRP Rebar with Enhanced Ductility and Sensing Capability," *Proceedings of the Fourth National Workshop on Bridge Research in Progress*, Buffalo, New York, June 1996, pp. 331-336.

4. Krishnamoorthy, R.K., Belarbi, A., Chandrashekhara, K., and Watkins, S., "Hybrid Composite Rebars for Smart Concrete Structures," *Proceedings of SPIE Smart Structures and Materials Conference*, Vol. 3043, March 1997, pp. 65-71.

5. Chang, C.C., Foedinger, R., Sirkis, J., and Vandiver, T., "Embedded Fiber Optic Sensor for Filament Wound Composite Structures," *Proceedings of the International Composites Expo* '97, Nashville, Tennessee, January 1997, pp. 19B1-19B6.

6. Krishnamoorthy, R.K., "Smart Pseudo-Ductile Composite Reinforcing Bars for Concrete," M.S. Thesis, University of Missouri - Rolla, August 1997, 69 pp.

7. Sutinjo, A.T., "Strain Measurement in Fiber Reinforced Plastic Composite Bars Using Fiber Optic Sensors," M.S. Thesis, University of Missouri - Rolla, August 1997, 71 pp.

8. Tamuzs, V., and Tepfers, R., "Ductility of Non-Metallic Hybrid Fiber Composite Reinforcement for Concrete," *Proceedings of the Second International RILEM Symposium*, Ghent, Belgium, August 1995, pp. 18-25.

9. Bakis, E.C., Nanni, A., and Terosky, J.A., "Smart, Pseudo-Ductile, Reinforcing Rods for Concrete: Manufacture and Test," *First International Conference on Composites in Infrastructure*, ICCI' 96, Tucson, Arizona, January 1996, pp. 95-108.

10. Harris, H.G., Somboonsong, W., Ko, F.K., and Huesgen, R., "A Second Generation Ductile Hybrid Fiber Reinforced Polymer (FRP) for Concrete Structures," *Second International Conference on Composites in Infrastructure*, ICCI'98, Tucson, Arizona, January 1998, pp. 66-79.

11. Jiang, C., "Manufacturing and Process Modeling of FRP Rebars By A Combined Pultrusion/Filament Winding Process," M.S. Thesis, University of Missouri - Rolla, January 1998, 50 pp.
12. Hamid, A.A., Saboni, A.R., and Mokhtar, A., "Flexural Behavior of One-Way Concrete Slabs Reinforced with GFRP Bars," *Second International Conference on Composites in Infrastructure*, ICCI'98, Tucson, Arizona, January 1998, pp. 15-23.

13. Taerwe, L. and Matthys, S., "Comparison of Concrete Slabs Pretensioned with Composite Bars and Steel Wires," *First International Conference on Composites in Infrastructure*, ICCI' 96, Tucson, Arizona, January 1996, pp. 506-519.

14. Razaqpur, A.G., and Ali, M.M., "A New Concept for Achieving Ductility in FRP-Reinforced Concrete," *First International Conference on Composites in Infrastructure*, ICCI' 96, Tucson, Arizona, January 1996, pp. 401-413.

15. Cosenza, E., Manfredi, G., and Realfonzo, R., "Behavior and Modeling of Bond of FRP Rebars to Concrete," *Journal of Composites for Construction*, May 1997, pp. 40-51.

16. Chang, C.C., Foedinger, R., Sirkis, J., and Vandiver, T., "Embedded Fiber Optic Sensor for Filament Wound Composite Structures," *Proceedings of the International Composites Expo '97*, Nashville, Tennessee, January 1997, pp. 19B1-19B6.

17. Malvar, L.J., and Bish, J., "Grip Effects in Tensile Testing of FRP Bars," *Proceedings of the Second International RILEM Symposium*, Ghent, Belgium, August 1995, pp. 108-115.

18. Park, R., and Paulay, T., *Reinforced Concrete Structures*, John Wiley & Sons, New York, 1975, 769 pp.

19. Tholen, M., and Darwin, D., "Effect of Reinforcing Bar Deformation Pattern on Flexural Ductility," *American Concrete Institute Structural Journal*, Vol. 95, No. 1, January-February 1998, pp. 37-42.

20. Naaman, A.E., and Jeong, S.M., "Structural Ductility of Concrete Beams Prestressed with FRP Tendons," *Non-Metallic (FRP) Reinforcement for Concrete Structures*, L. Taewere, ed., E & FN Spon, London, England, pp. 379-386.

21. R. M. Measures, "Advances Toward Fiber Optic Based Smart Structures," Optical Engineering, 31(1), pp. 34-47, 1992.

22. Eric Udd, Fiber Optic Smart Structures, (John Wiley and Sons, Inc., New York) 1995.

23. A. M. Vengsarker, K.A. Murphy, and M. F. Gunther, "Low Profile Fibers for Embedded Smart Structures Applications," Proceedings of SPIE, 2360, pp. 372-375 (1994).